2009 Hydrogen Program and Vehicle Technologies Annual Merit Review
and Peer Evaluation Meeting
Arlington, Virginia – May 18-22, 2009

Advanced Cathode Catalysts

Piotr Zelenay

Los Alamos National Laboratory
Los Alamos, New Mexico 87545

Project ID: FC_21_Zelenay

Overview

Timeline

- **Start date:** January 2007
- **End date:** Four-year duration

Budget

- **Total funding estimate:**
  - DOE share: $10,000K
  - Contractor share: $445K
- **FY08 funding received:** $2,894K
- **FY09 funding estimate:** $2,500K

Barriers

- **A. Durability** (catalyst; electrode)
- **B. Cost** (catalyst; MEA)
- **C. Electrode Performance** (ORR kinetics; O_2 mass transport)

Partners – Principal Investigators

Brookhaven National Laboratory

BROOKHAVEN NATIONAL LABORATORY – Radoslav Adzic

Argonne National Laboratory

Argonne NATIONAL LABORATORY – Debbie Myers

University of Illinois, Urbana

ILLINOIS UNIVERSITY OF ILLINOIS AT URBANA-CHAMPAIGN – Andrzej Wieckowski

University of New Mexico

The University of New Mexico – Plamen Atanassov

University of California, Riverside

UC RIVERSIDE UNIVERSITY OF CALIFORNIA – Yushan Yan

Cabot Fuel Cells

CABOT – Paolina Atanassova

Oak Ridge National Laboratory

ornl – Karren More

Relevance: Objective & Targets

Objective: Develop oxygen reduction reaction (ORR) catalysts alternative to pure Pt and electrode structures suitable for the new catalysts that together are capable of fulfilling cost, performance and durability requirements established by the DOE for the polymer electrolyte fuel cell cathode; also, assure path forward to large-scale fabrication of successful compositions.

Technical targets:

- **Platinum group metal loading:** 0.3 mg_{PGM}/cm^2 (both electrodes)
- **Activity** (PGM catalysts)**:** 0.44 A/mg_{Pt} at 0.90 $V_{iR\text{-}free}$ 720 $\mu A/cm^2$ at 0.90 $V_{iR\text{-}free}$
- **Activity** (non-PGM catalysts)**:** $>$ 130 A/cm^3 at 0.80 $V_{iR\text{-}free}$
- **Durability with cycling:** 5,000 hours at $T \leq 80°C$, 2,000 hours at $T > 80°C$
- **ESA loss:** $<$ 40%; **Cost:** $<$ 5 $/kW

Project impact in past year:

- **Developed a number of catalysts with much reduced Pt content, ORR activity exceeding DOE target, and very good RDE cycling durability**
- **Accomplished industrial scale-up of the first core-shell catalyst**
- **Demonstrated non-PGM catalysts with volumetric ORR activity on track to meeting the DOE 2010 target**

Approach: Focus Areas

- **Two classes of ORR catalysts** (down-selected from three classes initially)**:**
  - catalysts with ultra-low platinum content (stable metals or alloys as cores; non-precious-metal core catalysts; mixed metal shells for higher ORR activity)
  - non-precious metal catalysts (low- and high-temperature catalysts based on transition metals precursors)
- **Electrode-structure development:**
  - synthetic-carbon electrodes with hierarchical structure by emulsion/reverse-emulsion method
  - carbon- and non-carbon-based nanostructures for efficient mass transport, improved durability, and maximum catalyst utilization
  - modeling of non-precious metal catalyst layer in response to the mass-transport challenge in thick layers
- **Comprehensive catalyst characterization, active-site and ORR mechanism determination; modeling of oxygen reduction kinetics on non-precious metal catalysts**
- **Development of industrial scale-up methods for viable catalysts**

Approach: Milestones & Go/No-go Decision

DATE	MILESTONE	STATUS	COMMENTS
Dec 08	Achieve cathode performance of the $Pt_{ML}/Pd_3Fe/C$ electrocatalyst of 1.5 A/mg_{Pt} or 0.4 $A/mg_{(Pt+Pd)}$; determine durability of the catalyst.	**Partially complete**	1.1 A/mg_{Pt} achieved; reduction in particle size needed (future research)
Jan 09	Develop system for direct electrochemical detection of H_2O_2 in polymer electrolytes.	**Complete**	Prototype thin-gap system demonstrated and tested
Feb 09	Complete development of 1-3 nm Pt catalyst, dispersed within the hierarchical structure of a synthetic-carbon obtained using emulsion/reverse-emulsion method; assure performance of 0.15 A/mg_{Pt} at 0.9 V (iR-free).	**Partially complete**	3 nm particles & 0.10 A/mg_{Pt} at 0.9 V achieved; Gen II catalyst synthesized, ready for optimization and testing
Mar 09	Develop a method of step-wise growth of ideal Pt monolayer/bi-layer on various nanoparticles using a Cu-UPD-mediated growth to obtain gram-quantities of electrocatalysts.	**Complete**	Established using 2-gram batches; structure verified with HAADF-STEM imaging
Apr 09	Demonstrate two well-performing non-precious metal ORR catalysts supported on nanotubes/nanofibers; complete a comparative performance study of non-precious metal catalysts on dispersed and nanostructered supports.	**Pending**	Initial tests of PPy-nanotubes & catalyzed nanostructures completed; PANI-*Me*-CNT research ongoing
May 09	Develop the synthesis and demonstrate two chalcogenide catalysts with Ru replaced in at least 50% by transition metals other than Fe and with ORR activity comparable or higher than that of a reference Se/Ru/C catalyst.	**No-go**	Ru replacement, surface-chalcogenide class of catalyst abandoned (cf. a no-go decision below)
Aug 09	Double ORR activity of the best heat-treated and untreated heteroatomic polymer nanostructure catalysts in July 08.	**Complete**	FC performance at 0.80 V improved by at least 5 times
Sep 09	Determine the oxidation state, chemical composition, and stability of three advanced cathode catalyst classes as a function of potential and time using in situ and ex situ x-ray absorption spectroscopy and electrochemical measurements.	**Partially complete**	XAS data on four catalyst classes; one system fully analyzed; stability testing of PANI-Co-C system ongoing

Go/No-go: RDE tests yielding $E_{½}$ no-higher than 0.7 V vs. RHE for catalysts with Ru partially replaced by Ni, Fe, and Co; performance judged unsatisfactory. "No-go" for the replacement of Ru by transition metals and for the class of surface-chalcogenide catalysts.

H_2O_2 Detection in Absence of Liquid Electrolyte

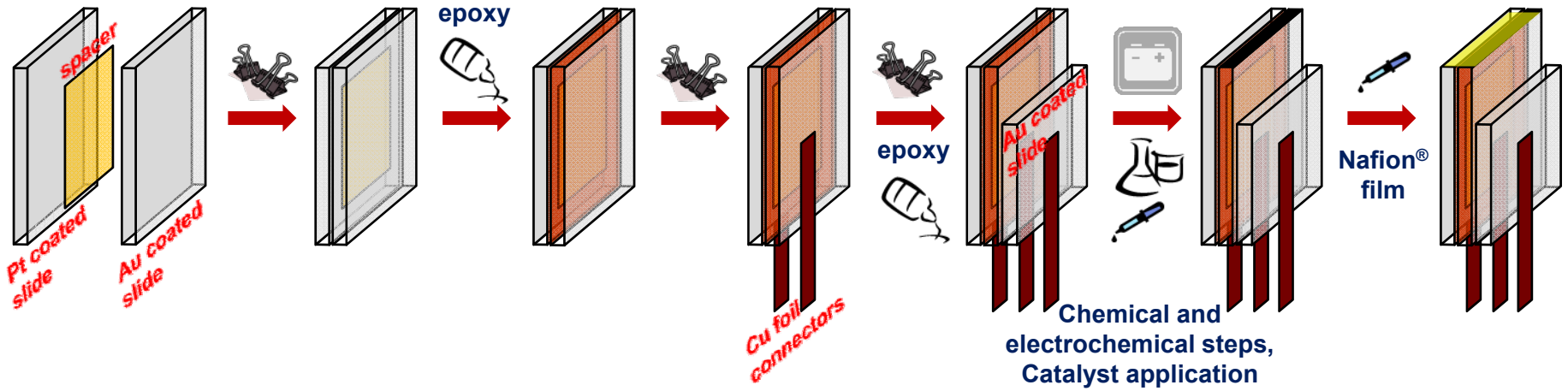

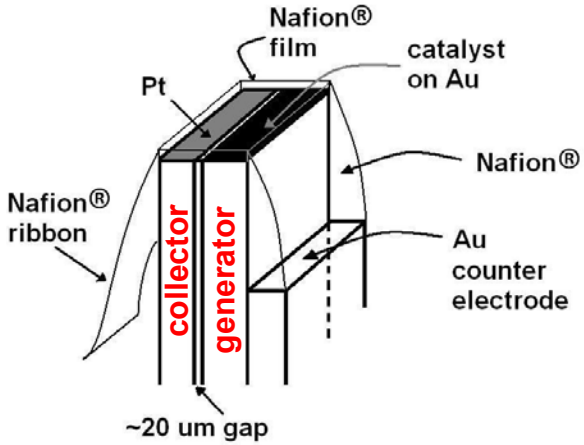

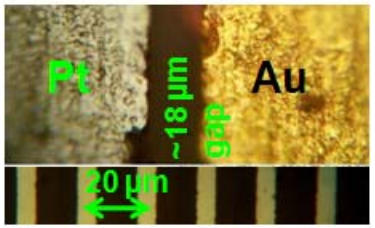

Co-PPy-XC72 (not heat-treated), 20° C

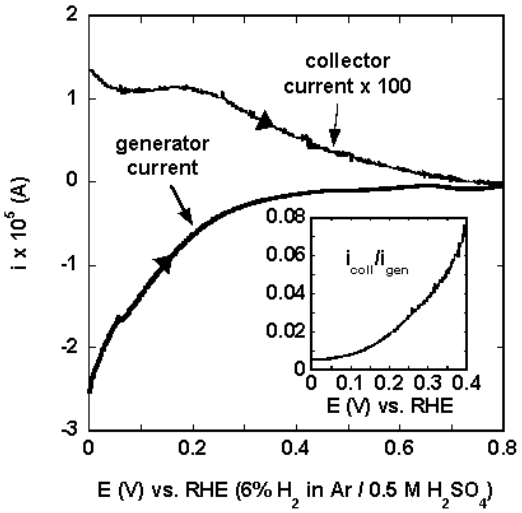

PANI-Fe-KJEC300J (heat-treated), 20° C

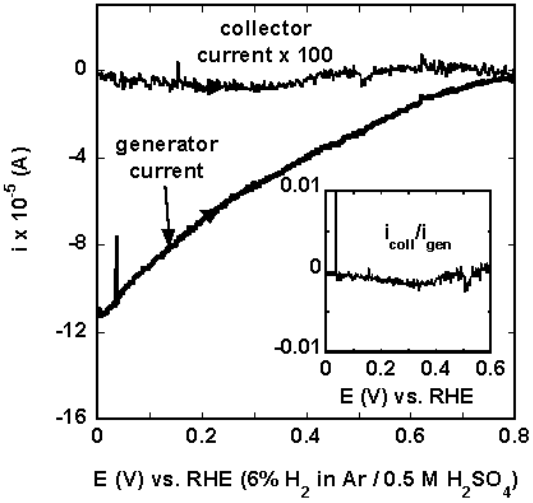

- Sensor for H_2O_2 detection in polymer electrolyte designed and built
- Significant differences in H_2O_2 generation detected with different catalysts

Sensor milestone achieved!

Ultra-low Pt Content Catalysts: Pd Interlayer Effect on ORR Activity

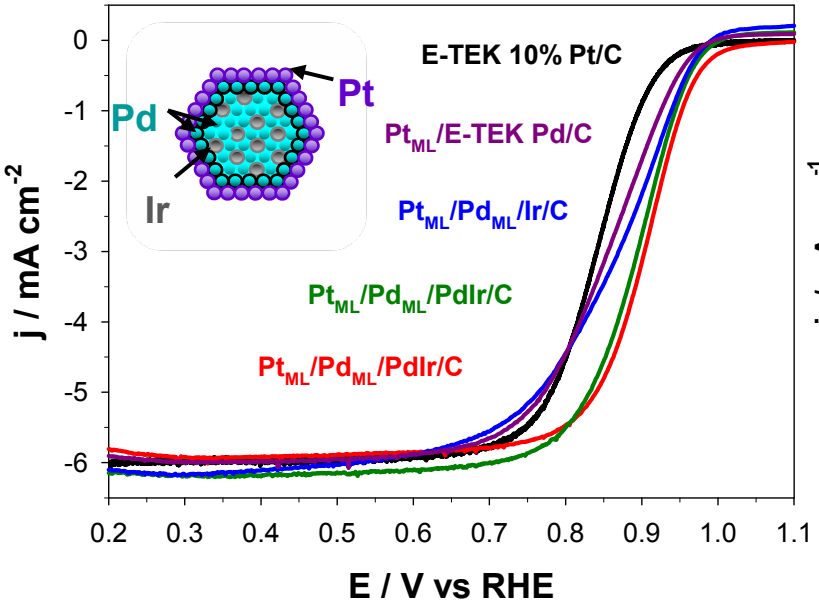

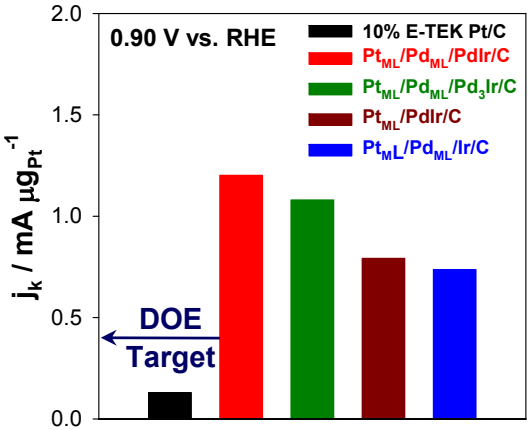

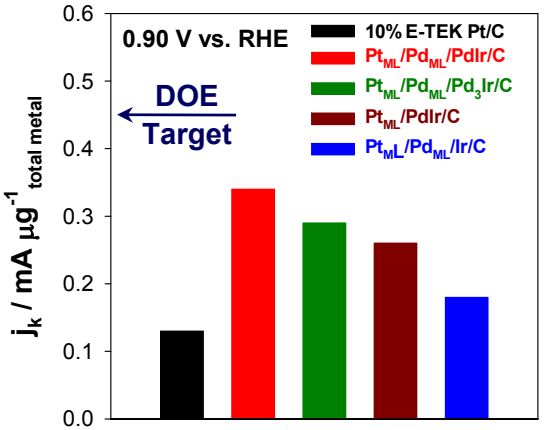

- **Highlight: 1.2 A/mg$_{Pt}$ at 0.90 V – an improvement of 0.4 A/mg$_{Pt}$ due to Pd interlayer (better lattice constant for Pt overlayer)**
- **Highlight: $E_{1/2}$ loss after 30,000 cycles of only 19 mV *vs.* 39 mV for Pt/C**
- **Pd not significantly oxidized (XAS); good substrate for Pt compared to other metals, e.g. iridium**

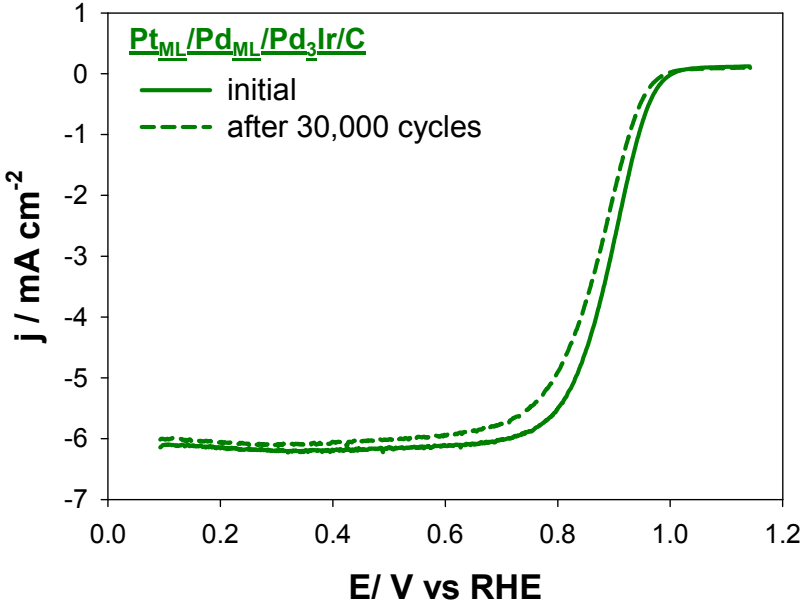

Ultra-low Pt Content Catalysts: Improved Durability

Stability test for 600°C-annealed $PtAu_{0.12}/C$ (8 nm, Johnson Matthey)

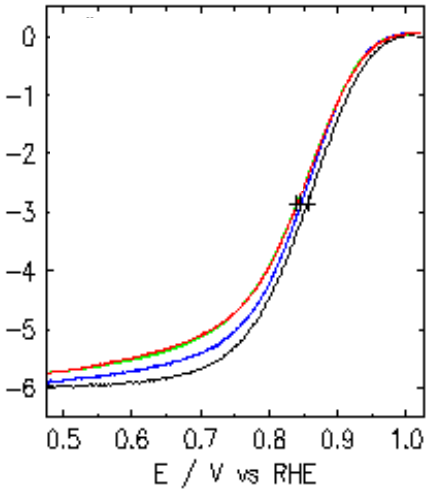

$PtAu_{0.12}/C$ (8-nm, JM)		
# cycles	$E_{1/2}$ (V)	$\Delta E_{1/2}$ (mV)
Initial	0.856	n/a
20,000	0.846	10
30,000	0.840	16
50,000	0.840	16

40 wt% Pt/C (8-nm, JM)		
# cycles	$E_{1/2}$ (V)	$\Delta E_{1/2}$ (mV)
Initial	0.867	n/a
20,000	0.830	37
30,000	0.825	43
n/a	n/a	n/a

- **Highlight**: Au clusters on Pt/C reducing $\Delta E_{1/2}$ after 30,000 cycles from 43 mV to 16 mV; no further $E_{1/2}$ shift with 50,000 cycles
- Pt loading 30 μg cm^{-2}; nominal Au coverage: 0.6 monolayer
- Potential cycle: 0.95-0.70 V (30 s intervals) in air at 23°C

Stability test for $Pt/Pd_3Fe/C$ (new synthesis)

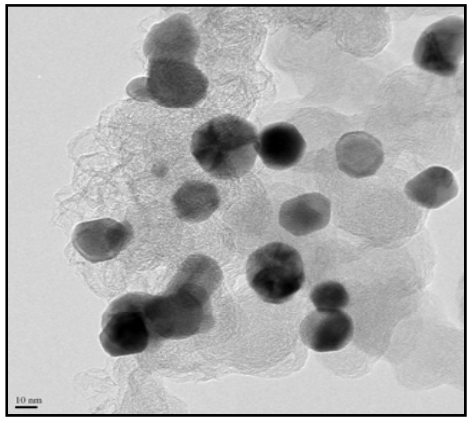

TEM of Pd_3Fe/C

(XRD: well-alloyed, ~ 10 nm)

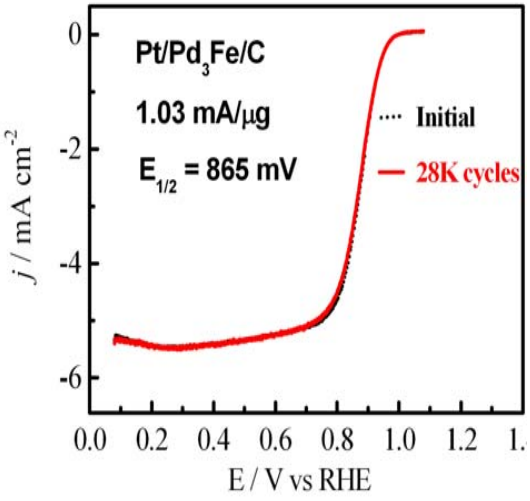

- **Highlight**: Remarkable durability of $Pt/Pd_3Fe/C$ catalyst - $\Delta E_{1/2}$ < 5 mV after 28,000 cycles
- No Fe dissolution observed in cyclic voltammetry
- Potential cycle: 0.95-0.70 V (30 s intervals) in air at 23°C

Ultra-low Pt Content Catalysts: Scale-up Synthesis

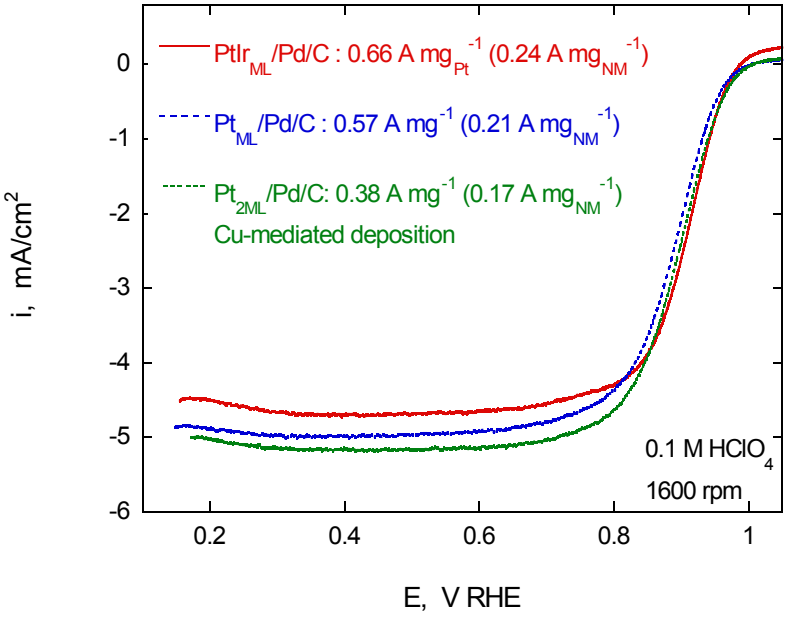

XAS verification of $Pt_{80}Ir_{20}$ monolayer composition

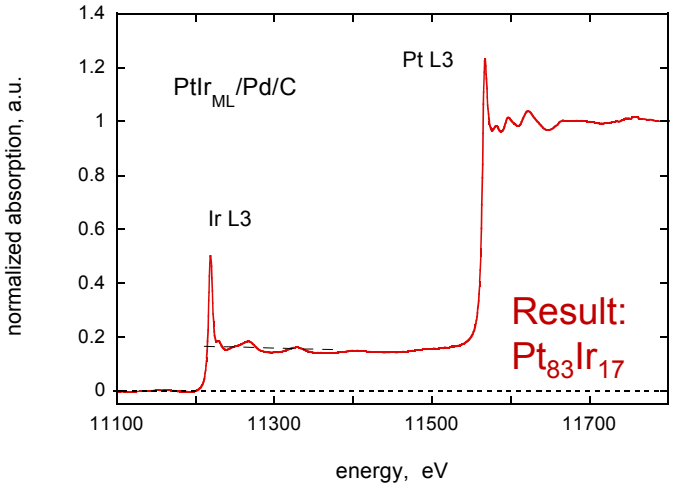

Verification of core-shell structure: HAADF-STEM images with (3D) atomic structure modeling

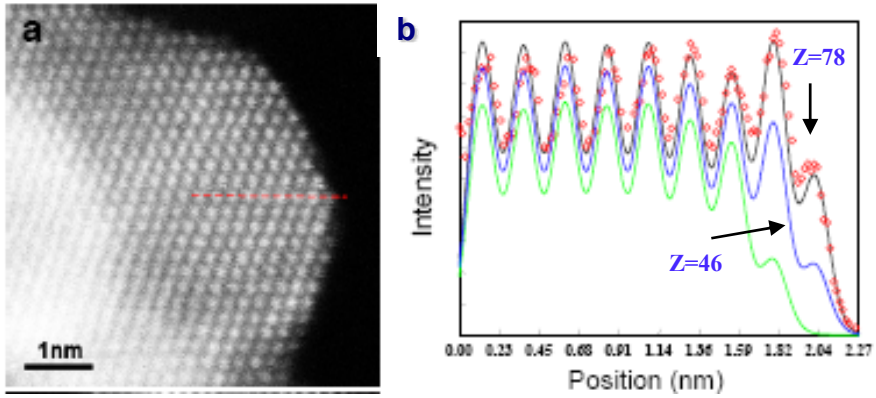

Best model fit to structure: Pt ML + Pd ML + core

- **Highlight: High activity from scale-up synthesis**
  - **PtIr/Pd/C – 0.24 A/mg$_{PGM}$ or 0.66 A/mg$_{Pt}$**
  - **Pt/Pd/C – 0.21 A/mg$_{PGM}$ or 0.57 A/mg$_{Pt}$**
  - ***Scale-up milestone achieved!***
- **Highlight: Scale-up to 5 grams in a single batch demonstrated by two methods (Cu-UPD displacement and Cu-UPD-mediated layer-by-layer growth)**
- **Composition confirmed by ICP and XAS**
- **Core-shell structure verified by HAADF-STEM images and modeling**

Industrial Scale-up: Synthesis of Highly-Active Pt/Pd/C Catalyst

Anode: *0.05 mg_{Pt} cm^{-2}, 1.5 H_2 at 1 A/cm^2* ***Cathode:*** *2.5 air at 1 A/cm^2* ***Conditions:*** *50 cm^2 MEA, 80 ° C, 100% RH, 30 psig, 10 min/point step* ***Membrane:*** *Nafion® 212*

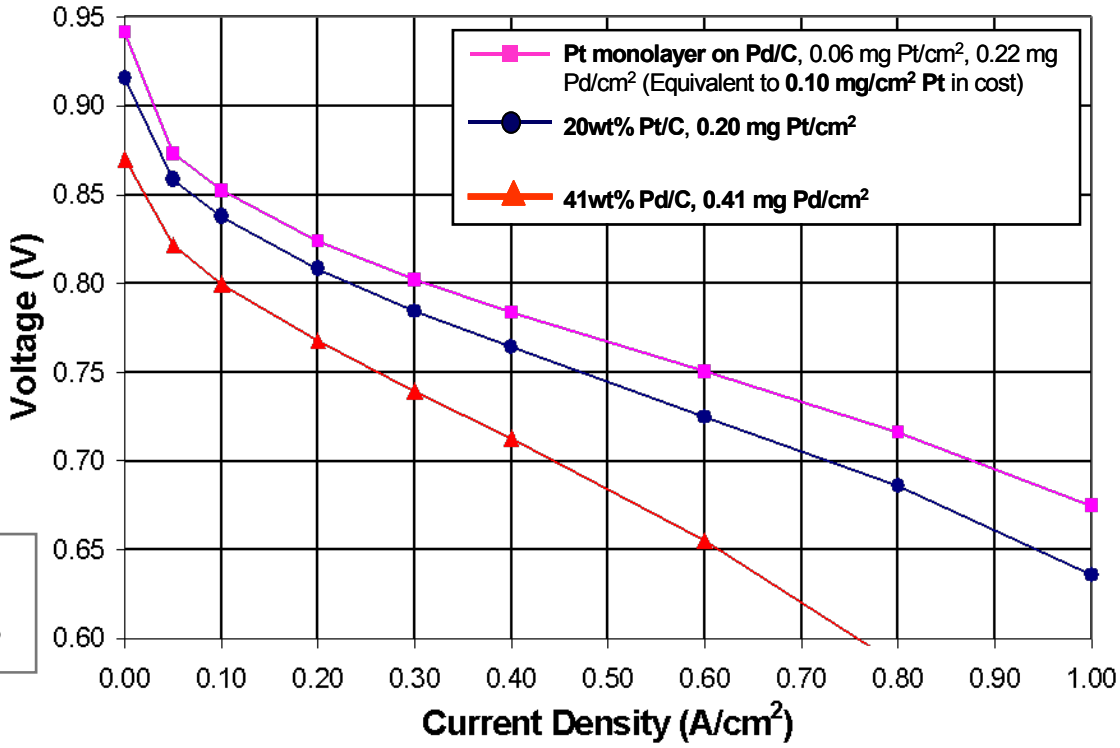

- **Pt/Pd/C – the first catalyst selected for scale-up from Brookhaven NL part of project**
- **Highlight: Pt_{ML}/Pd/C catalyst, scaled-up in gram quantities, delivering excellent MEA performance at 0.90 V:**

0.55 A/mg_{Pt} vs. 0.08 A mg_{Pt} for MEA with Pt/C cathode; 0.12 A/mg_{Pt+Pd}

(data uncorrected for *iR*-losses or H_2 crossover)

Industrial scale-up of the first catalyst accomplished with very high ORR activity!

Non-precious Metal Catalysts

Composite catalysts derived from heteroatomic organic precursors (e.g. polyaniline - PANI, polypyrrole - PPy, cyanamide - CM, etc.), transition metals, and carbon; heat-treated at 600°C-1100 °C; and subjected to post-synthesis purification and activation steps

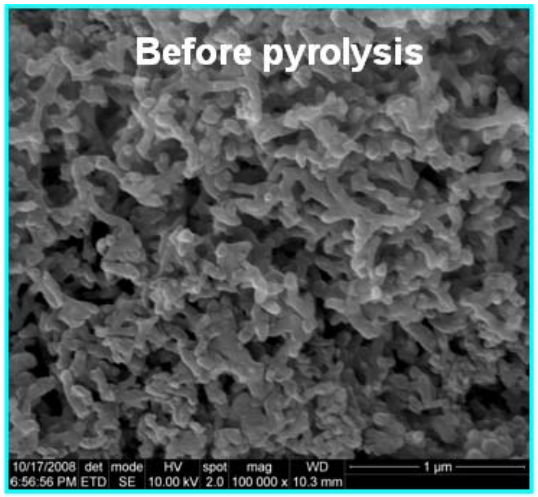

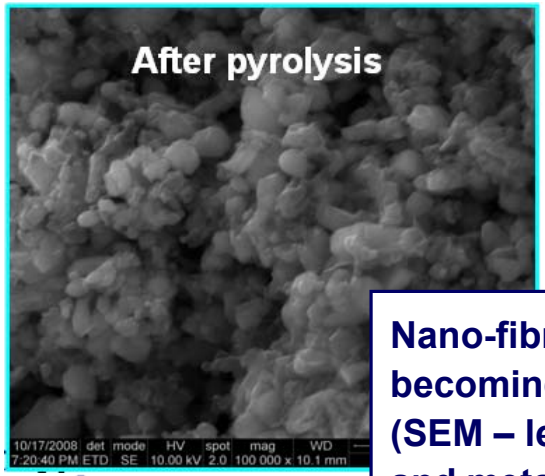

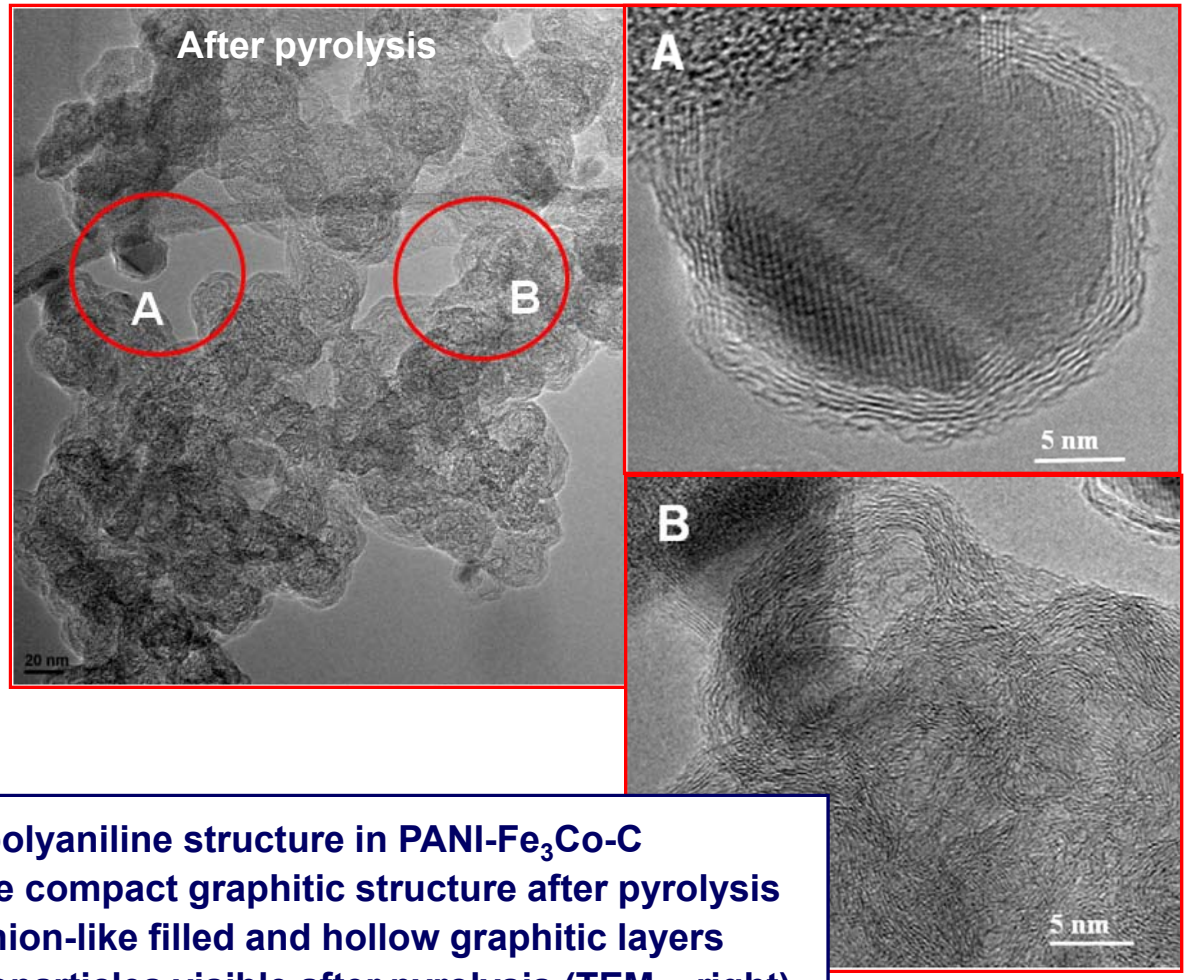

Nano-fibrous polyaniline structure in PANI-Fe_3Co-C becoming more compact graphitic structure after pyrolysis (SEM – left); onion-like filled and hollow graphitic layers and metal nanoparticles visible after pyrolysis (TEM – right).

PANI-derived Catalysts: Activation and RDE Performance

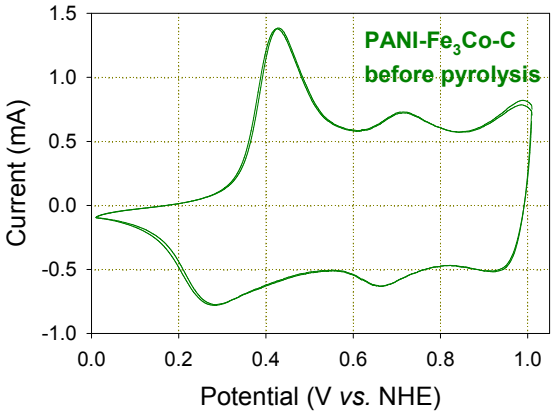

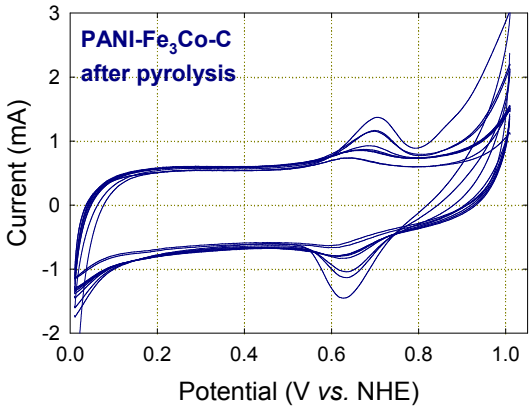

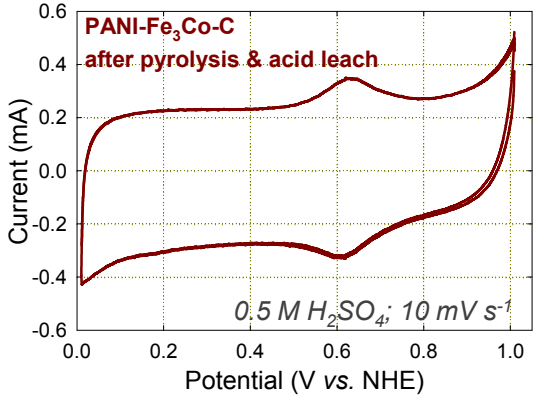

RDE & RRDE: *0.12 mg cm^{-2}; 0.5 M H_2SO_4; 5 mV s^{-1}; 900 rpm; 25 ° C; Ag/AgCl, (3 M NaCl) RE; Au-mesh CE*

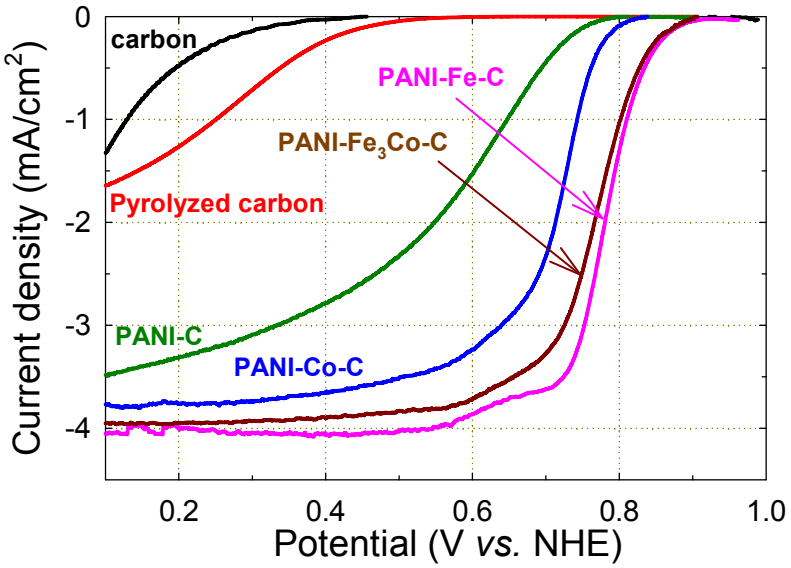

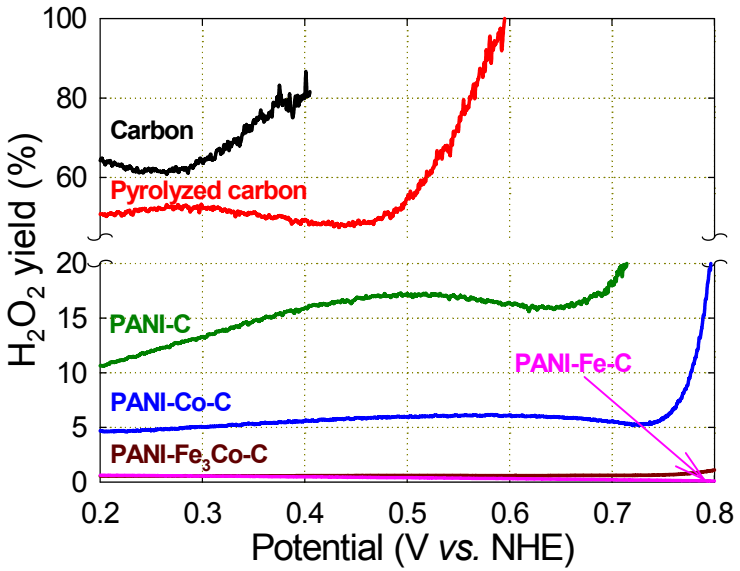

- **Stable voltammetry after pyrolysis and acid leach**
- **Highlight: ORR onset at E ≥ 0.9 V; $E_{½}$ ~0.77 V; H_2O_2 generation less than 0.5%**

PANI-Derived Catalysts: Electrochemical and XPS Characterization

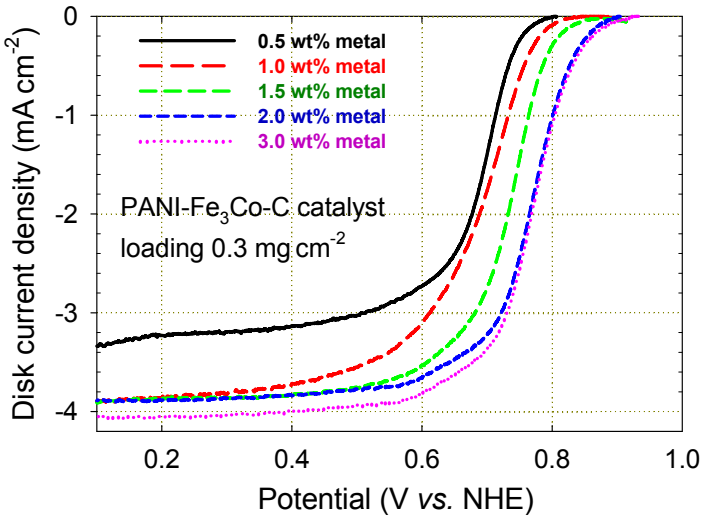

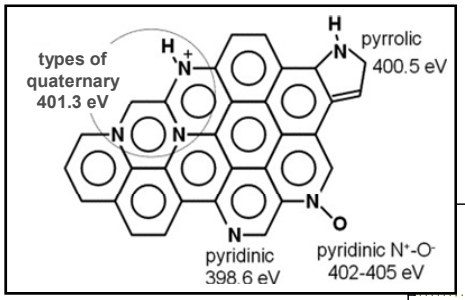

N 1s XPS spectra

The University of New Mexico

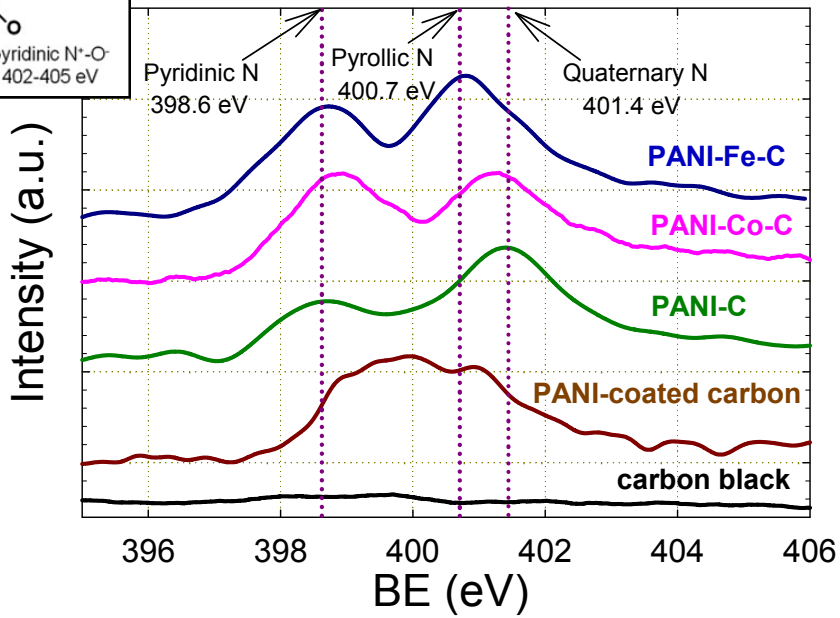

RDE: *0.5 M H_2SO_4; 5 mV s^{-1}; 900 rpm (unless otherwise indicated); 25 ° C; Ag/AgCl, (3 M NaCl) RE; carbon-rod CE*

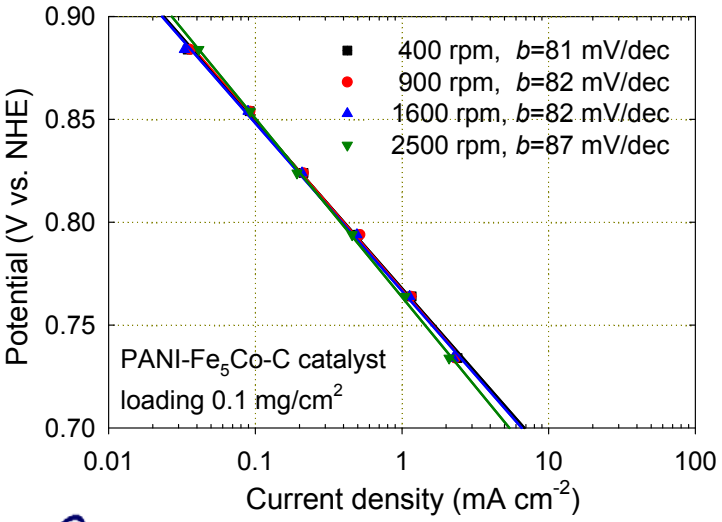

- **Activity increase with amount of Fe suggesting metal participation in active site formation and/or ORR itself**
- **ORR Tafel 80-90 mV/decade for Fe-based catalysts and (~75 mV/decade for Co-based catalysts, not shown)**
- **Highlight: Fe likely stabilizing pyrrolic N – possible cause of higher activity of Fe-based catalysts relative to Co-based ones; pyridinic N present in all active catalysts**

Los Alamos NATIONAL LABORATORY

Mechanistic Analysis of ORR Kinetic Data

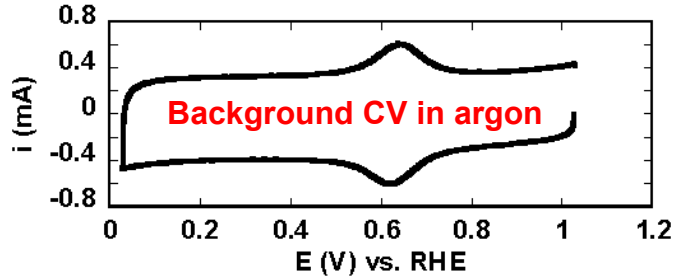

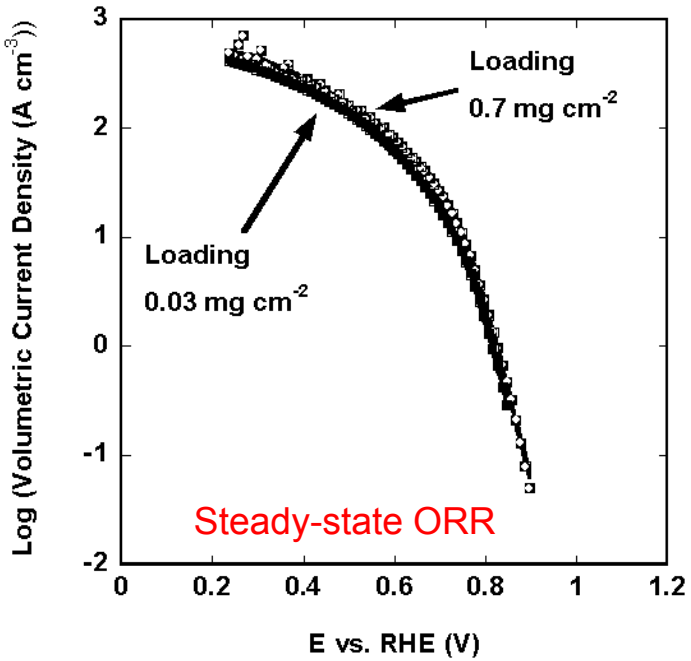

Ox + e^- ⇔ Red — $k_{fwd} = k_s \exp[-\alpha F(E-E°)/RT]$; $k_{bw} = k_s \exp[(1-\alpha)F(E-E°)/RT]$

↓

Red + O_2 + H^+ → Ox + (HO_2) * — rds (k_{chem} - rate constant)

↓

(HO_2)* + $3e^-$ + $3H^+$ → $2H_2O$ — fast reaction

Fitting equation:

$\log (i) = \log(nFA\Gamma k) + \log\{\{\exp[-\alpha F(E-E°)/RT]/\{\exp[-\alpha F(E-E°)/RT] + (k/k_s) + \exp[(1-\alpha)F(E-E°)/RT]\}\}$

Γ - surface concentration of mediator sites ($\Gamma = \Gamma_{red} + \Gamma_{ox}$)
$k = k_{chem} C_{H+} C_{O2}$; A - real catalyst surface area;
n - number of electrons exchanged in ORR

Average parameter values obtained:

$\alpha = 0.25$; $k/k_s = 12.6$; $E° = 0.662$ V
(E° measured for the reversible surface system - 0.646 V)

- **Variable Tafel slopes in RDE experiments unrelated to catalyst-layer porosity**
- **Intrinsic catalytic properties of the PANI catalyst responsible for the Tafel plot curvature**
- **Highlight: ORR likely mediated by a fast red-ox system on the catalyst surface**

Fe-PANI-C Catalyst: In-situ XAFS During Pyrolysis

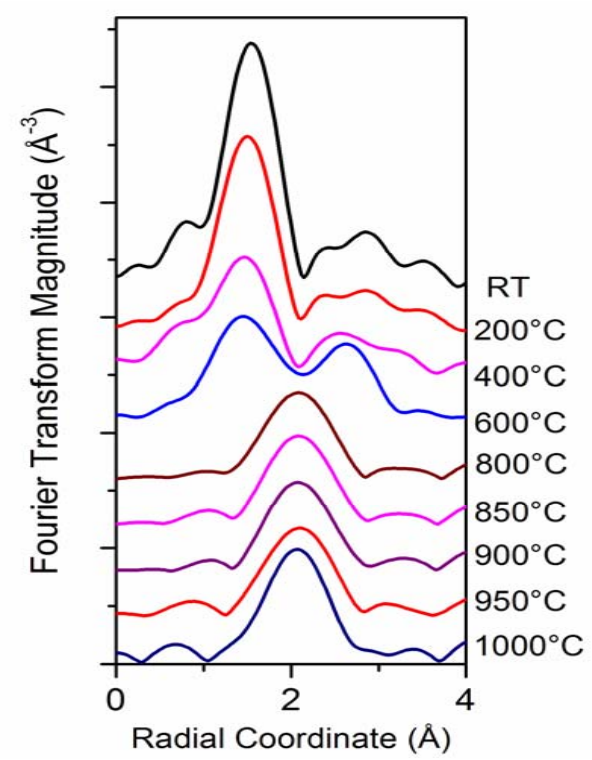

Temperature	Best Match to Spectra
RT, 200°C	Fe chloride
400°C	Fe sulfate/sulfide
600°C	Mixed Fe oxides (FeO, Fe_3O_4) and metallic Fe
800-1000°C	Reduced iron • metallic Fe with Fe carbides and sulfides • evidence of sintering at 1000°C

- **Highlight: Chemical changes due to pyrolysis observed; $FeCl_3$ at room temperature becomes Fe^0, Fe carbides, and sulfides at 800-1000°C**
- **Effect of varying precursors addressed in future**
- **Gas products: oxygen-containing species no longer detected above 800°C; most removed by 600°C**

Analysis of gas products of pyrolysis

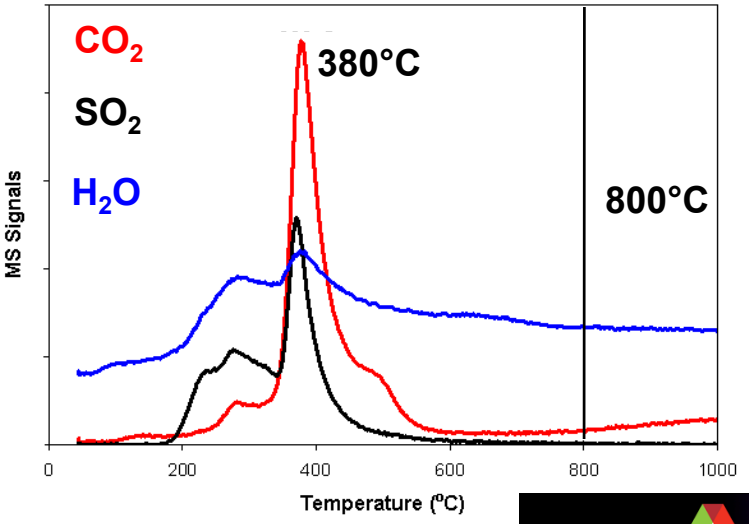

Fe-PANI-C Catalyst: Evolution of Fe in Catalyst (in-situ XAFS in Aqueous Cell)

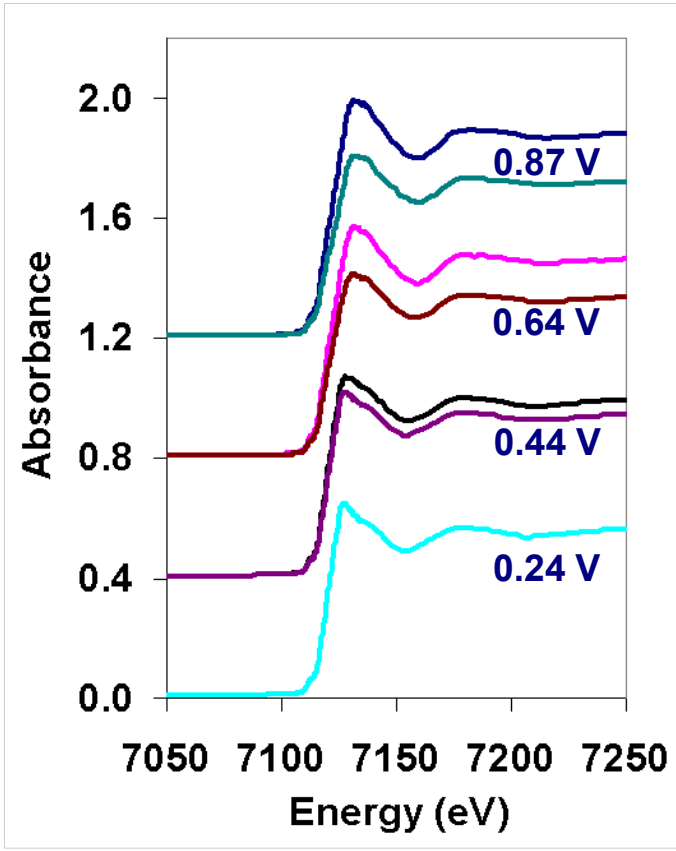

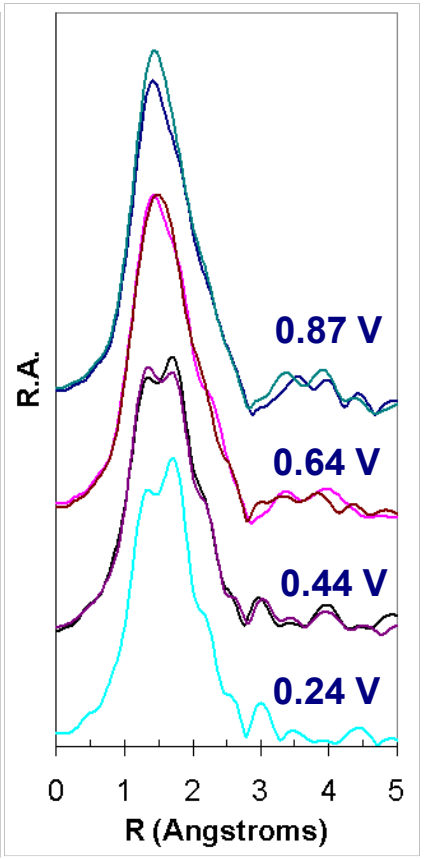

History	Fe wt%
Before pyrolysis	13
After pyrolysis	32
After pyrolysis and acid treatment	3.3
In fresh MEA	3.7
In MEA after 200 hr at 0.6 V	0.95

- **Reversible reduction of Fe^{3+} catalyst component between 0.64 and 0.44 V observed by XAFS**
- **Greatest loss of Fe from electrode observed during this reduction step (30% loss total)**
- **Highlight: Catalyst activity not decreasing concomitantly with loss of majority of Fe; minority Fe species considered for active site, or non-metal catalytic sites, or both**

Catalyst Surface Characterization by XANES at Transition Metal L-edge

- **Presence of Co signals (top) and Fe signals (bottom) in both total electron yield (TEY) and photon yield spectra of PANI-based catalysts indicating location of Co and Fe in these catalysts very close to or on the catalyst surface**
- Contrary to PANI-based catalysts, Fe in PPy-based catalyst not occupying the catalyst surface – as indicated by presence of Fe signals in the photon yield spectra (bottom left) and lack of them in TEY spectra (bottom right)
- **Participation of metal centers in the catalytic activity of PANI-based catalysts cannot be excluded**
- Catalytic activity of Fe-PPy catalyst resulting from the presence of non-metal surface sites
- **Highlight: L-edge XANES – much better surface specificity than with K-edge absorption spectroscopy**

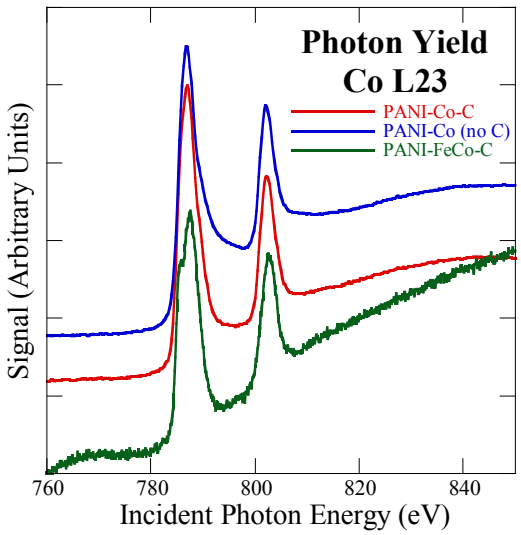

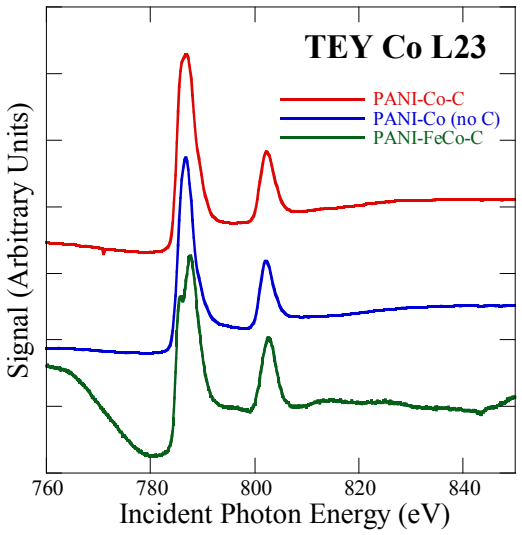

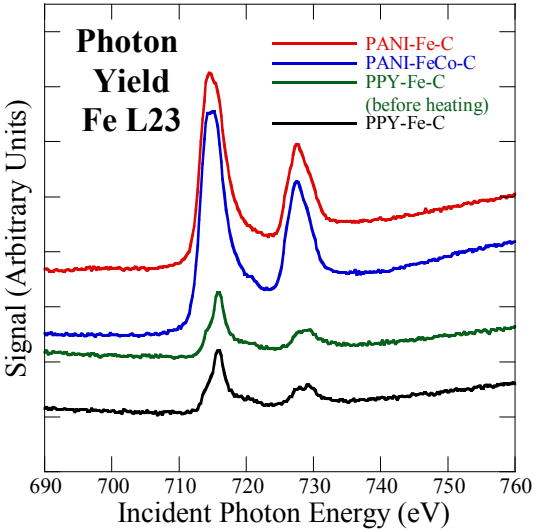

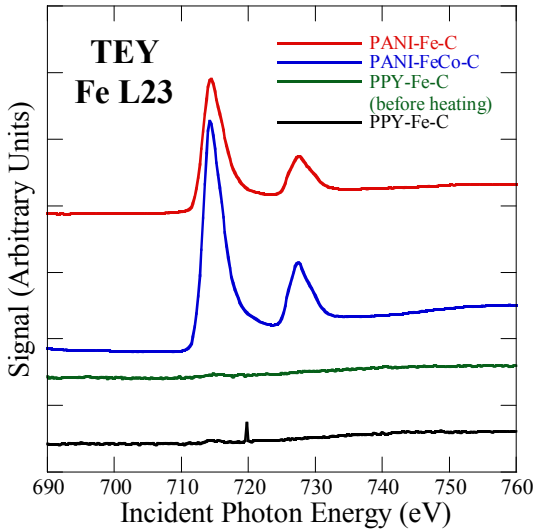

PANI-Fe_3Co-C Catalyst: Fuel Cell Performance

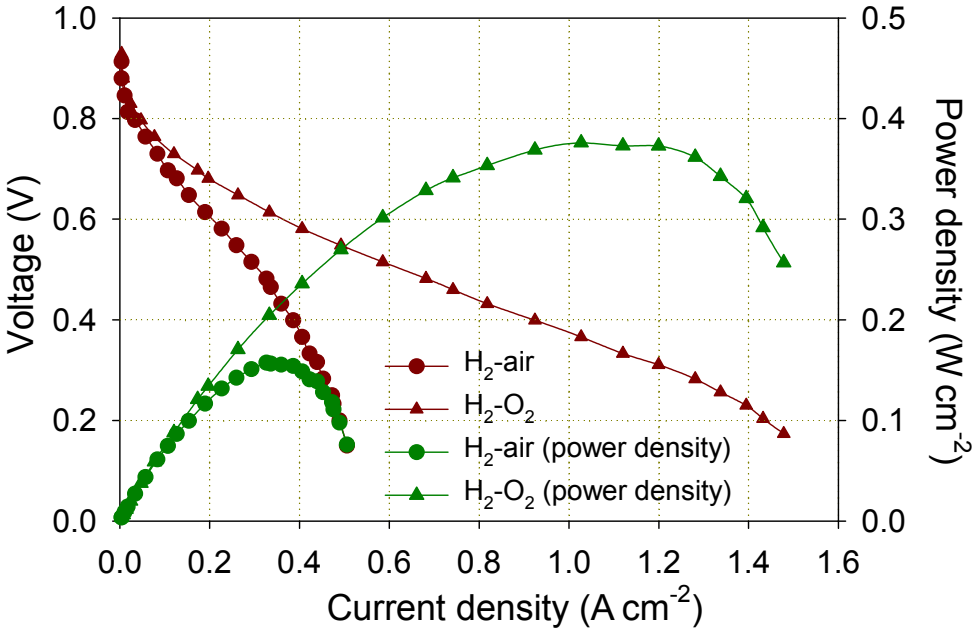

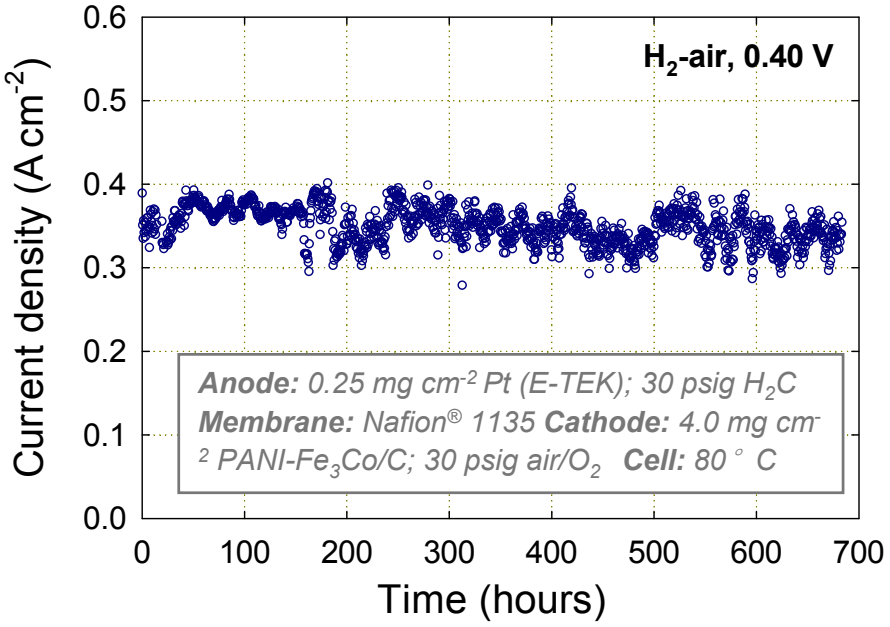

- **Highlight: High activity of PANI-Fe_3Co-C found in RDE experiments confirmed in fuel cell testing, both on air and oxygen:**

OCV (V): 0.91 (air)	$i_{0.80\ V}$ **(A cm^{-2}): 0.037** (air)	$i_{0.80\ V}$ **(A cm^{-3}): 19** (air)
0.93 (O_2)	**0.054** (O_2)	**27** (O_2)

iR-corrected data

- **Highlight: Little performance loss observed for nearly 700 hours of operation at 0.4 V**

Activity improvement milestone completed, significantly exceeded at 0.80 V (by a factor of ~ 5) and combined with respectable stability in long-term testing on air!

Cyanamide-Fe-C Catalyst: Performance

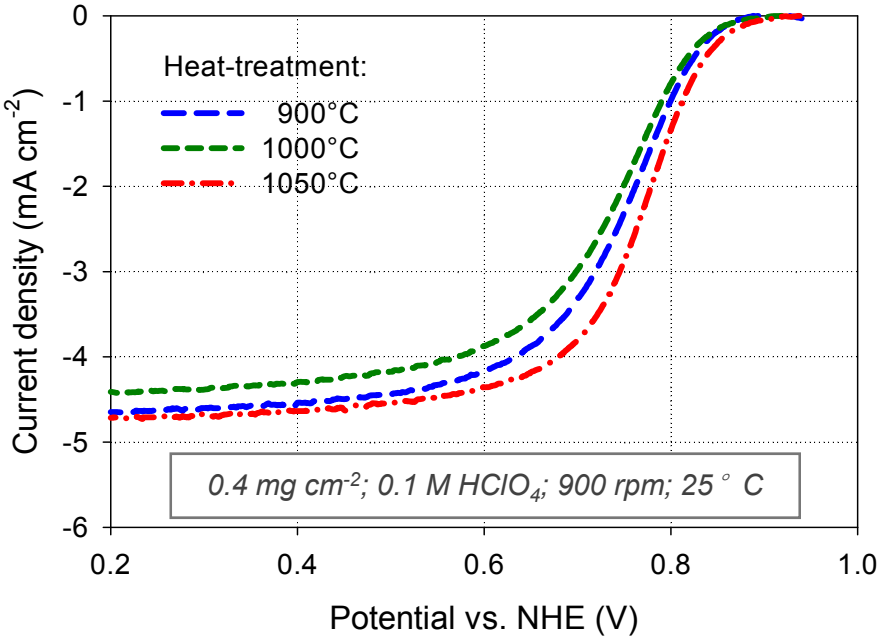

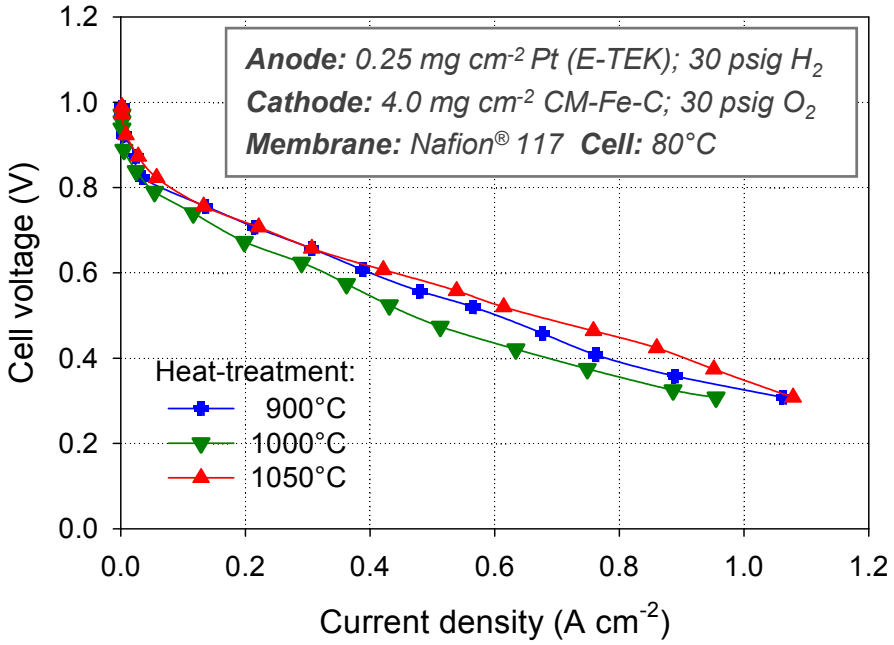

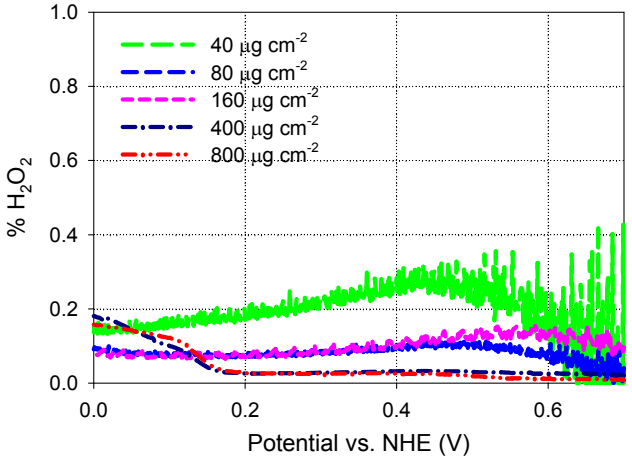

- **Highlight: Very high open cell voltage (OCV) of ~1.0 V obtained with CM-Fe-C catalysts, heat-treated at 1050°C and 900°C for one hour.**
- **High ORR activity accompanied by low peroxide yields, even at the lowest loading tested (40 µg cm^{-2})**
- **Highlight: 0.108 A cm^{-2} reached at 0.80 V in fuel cell testing; translating to volumetric activity of 54 A cm^{-3}** (*iR*-corrected)

  Two-fold activity improvement milestone completed and significantly exceeded at 0.80 V (by a factor of ~ 11)!
- **Stability of CM-Fe-C catalysts in need of improvement**

Towards Fe-free Catalysts: PANI-Co-C Catalyst; Other Options

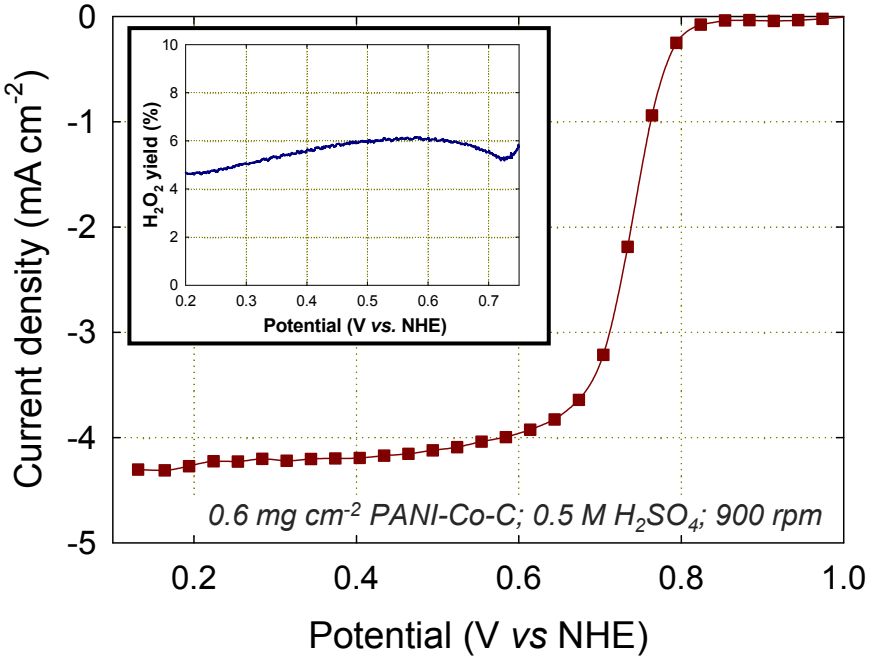

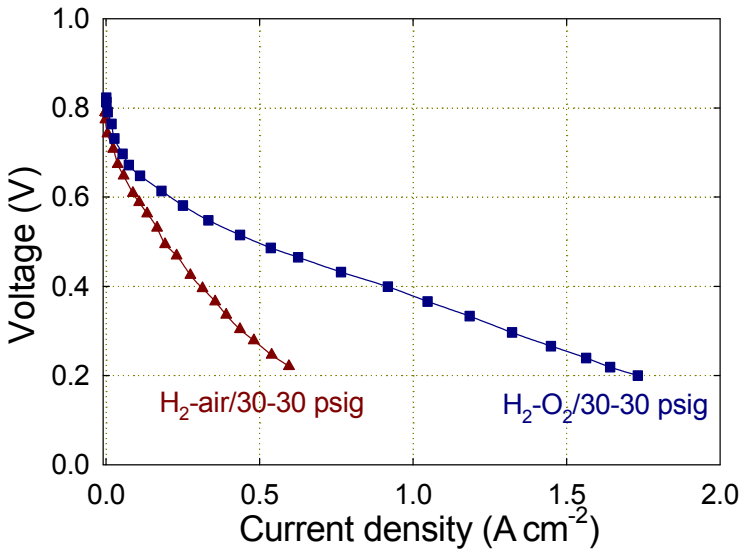

Anode: *0.25 mg cm^{-2} Pt; 30 psig H_2* ***Membrane:*** *Nafion® 1135*
Cathode: *4.0 mg cm^{-2} PANI-Co-C; 30 psig O_2/air* ***Cell:*** *80 ° C*

- **Although below performance of Fe-based PANI catalysts, PANI-Co-C offering promising activity and moderate peroxide yields**
- **Highlight: Good stability of PANI-Co-C catalyst**
- **Alternative approaches to minimizing possible detrimental role of iron:**
  - ✓ **Fe removal by aggressive leach, complexing, *etc.***
  - ✓ **Use of OH· scavengers, e.g. Ce^{3+} (Asahi Glass, GM approaches)**

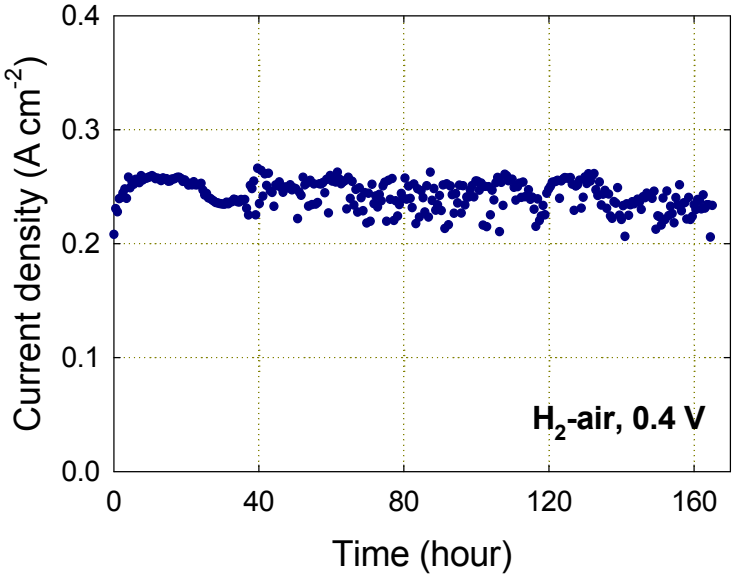

New Nanotube-supported Catalysts: Synthesis, Characterization, and Testing

Pt/MWNTs

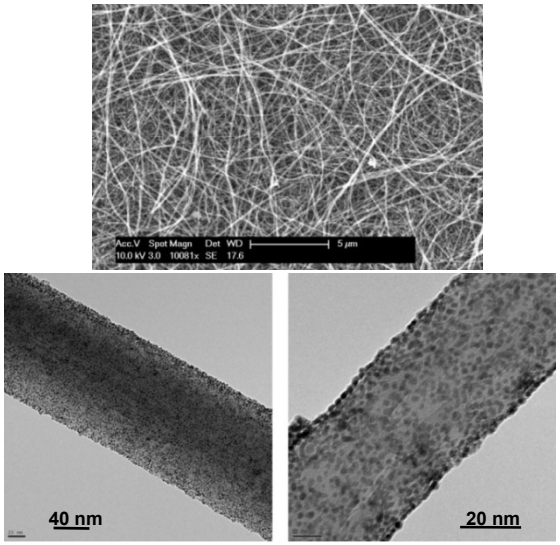

MEA fabrication

1 - Filtration

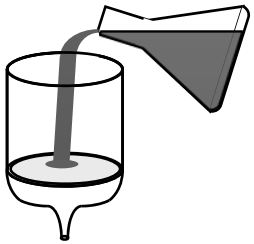

to vacuum flask

2 - Hot-pressing

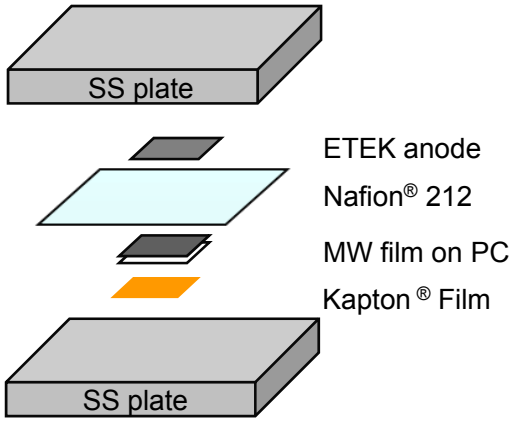

Anode: 0.2 mg_{Pt} cm^{-2}, 0.2 L/min H_2, 35 psig *Cathode:* 0.2 L/min air, 35 psig
Conditions: 5 cm^2 MEA, 70 ° C, 100% RH *Membrane:* Nafion® 212

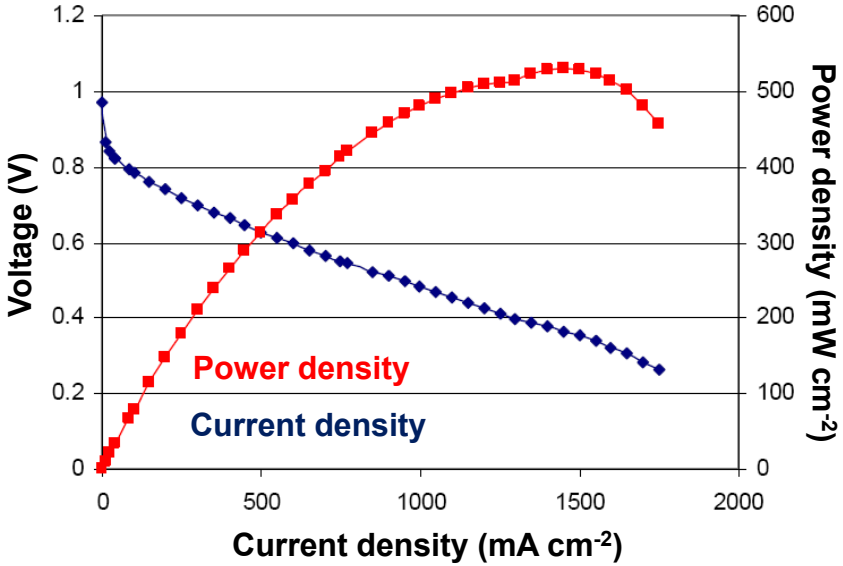

- **Highlight: Multi-walled carbon nanotubes (MWNTs) with unusually long length (~300 μm) developed, catalyzed, and incorporated into MEAs**
- **MWNT-supported cathode tested: 12 μg_{Pt} cm^{-2}, 30 wt% Pt/MWCNT, no Nafion®**
- **Good performance from MEAs on a per mg_{Pt} basis (at 0.90 V: 0.75 A $mg_{Pt\ cathode}$); overall performance in need of improvement**
- **Replacement of Pt with non-precious PANI-derived catalyst pending**

Silica-derived Electrode Structures: Control of Hierarchical Porosity

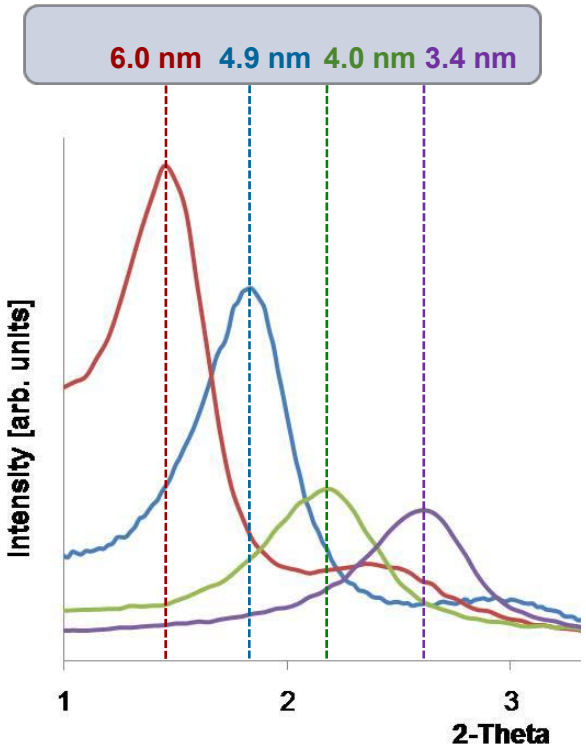

Properties of Silica Templates

Surfactant	BET, m^2/g	Pore size, nm
$CH_3(CH_2)_{17}N(Br)(CH_3)_3$	873	6.0
Standard, $CH_3(CH_2)_{15}N(Br)(CH_3)_3$	1000	4.9
$CH_3(CH_2)_{13}N(Br)(CH_3)_3$	1136	4.0
$CH_3(CH_2)_{11}N(Br)(CH_3)_3$	1198	3.4
$CH_3(CH_2)_9N(Br)(CH_3)_3$	↓ increase predicted	↓ decrease predicted
$CH_3(CH_2)_7N(Br)(CH_3)_3$		
$CH_3(CH_2)_5N(Br)(CH_3)_3$		

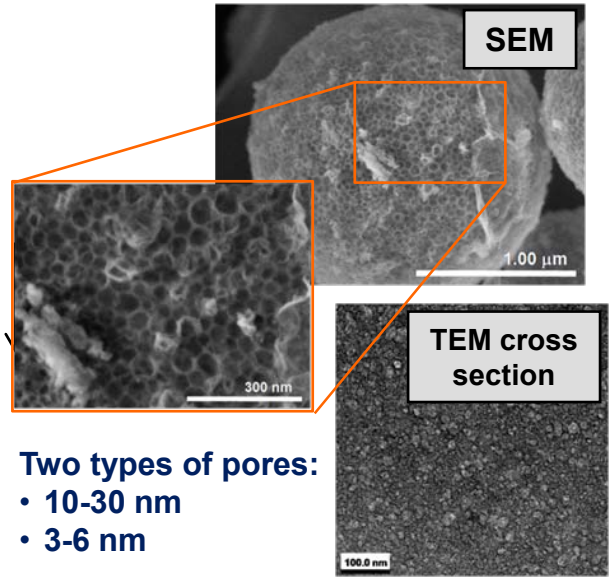

Two types of pores:
- **10-30 nm**
- **3-6 nm**

- **Highlight: Development of silica template with pores in 3-6 nm range for Pt particle size control and, possibly, enhanced durability**
- **Path forward to smaller pore size through the use of different surfactants (table)**
- **RDE experiments now reflecting expected performance; two-step pyrolysis introduced; MEA testing of second generation catalysts underway**

Properties of Non-precious Metal Catalyst Layer

X-ray tomography of a PANI-Fe_3Co-C MEA

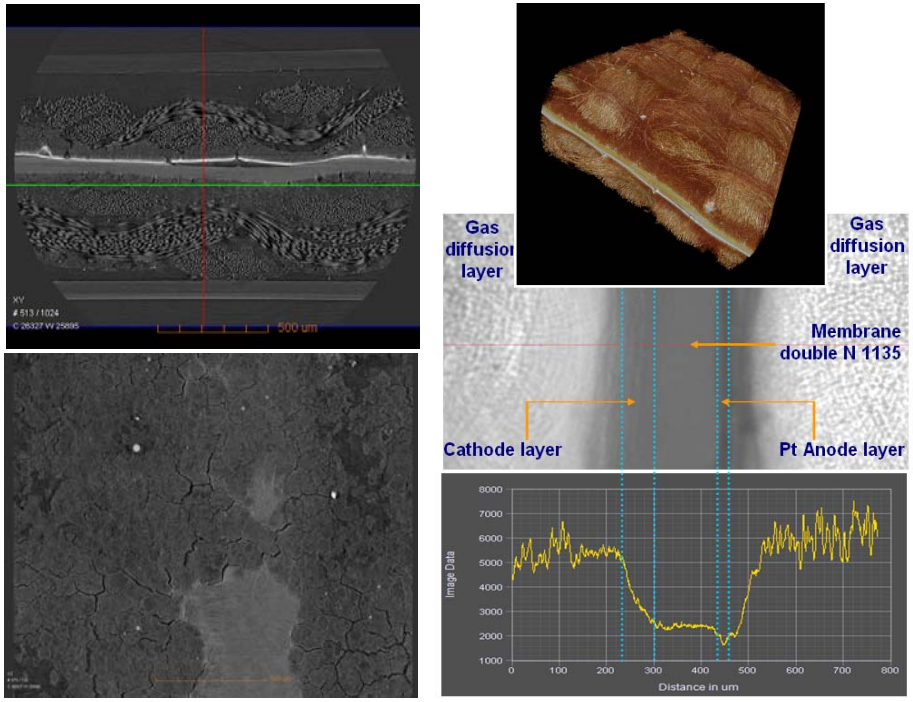

ΔE *vs. j* analysis of O_2 transport losses (PANI-Fe_3Co-C)

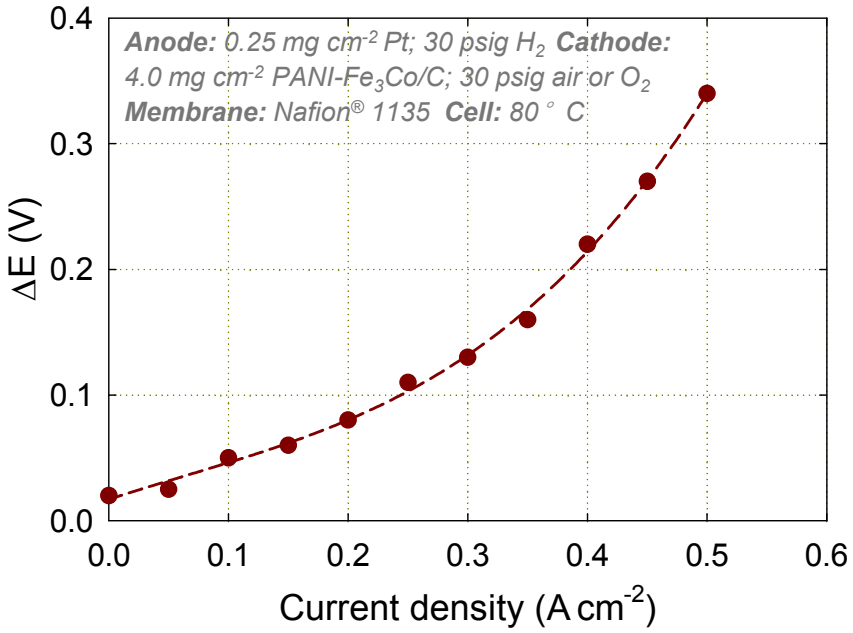

- **X-ray tomography revealing thick catalytic layer (~ 60 μm for PANI-derived catalysts at 4 mg cm^{-2})**
- **Significant transport hindrance – a major challenge of non-precious metal electrocatalysis**

Difference in fuel cell cathode performance on O_2 relative to air:

$$\Delta E = E_{O_2}(j) - E_{air}(j) = \frac{RT}{\alpha z F}\left(\ln\frac{P_{O_2}}{P_{air}} + \ln\frac{f_{O_2}(j)}{f_{air}(j)}\right)$$

f – electrode "efficiency" factor

Model of Non-precious Metal Catalyst Electrode (In Progress)

1. One-dimensional, macroscopic water and heat balance model under development
2. Focus on water evaporation and capillarity to understand flooding of thick catalyst layer
3. Developing mitigation strategies, i.e. through enhanced evaporation (model details in *Supplemental Slides*)

Liquid water transport equation:

$$-\frac{1}{V_m \mu^l}\frac{d}{dz}\left[K^l(S_r)\frac{dp_l(z)}{dz}\right] = S^l_{ORR} - S_{evap}(S_r)$$

Heat balance equation:

$$q_{tot} - q_{GDL} = h_{fg} J^{GDL}_{H_2O}$$

Modeling approach:

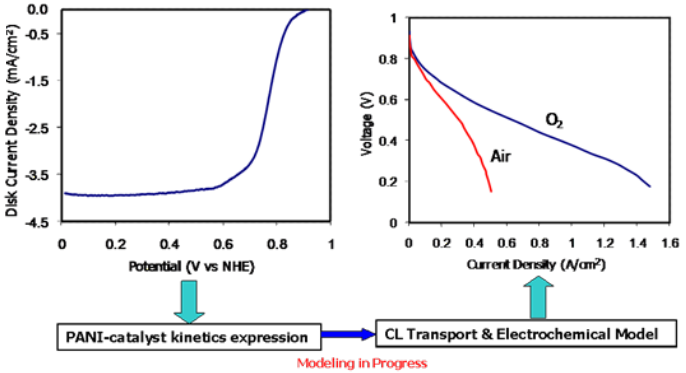

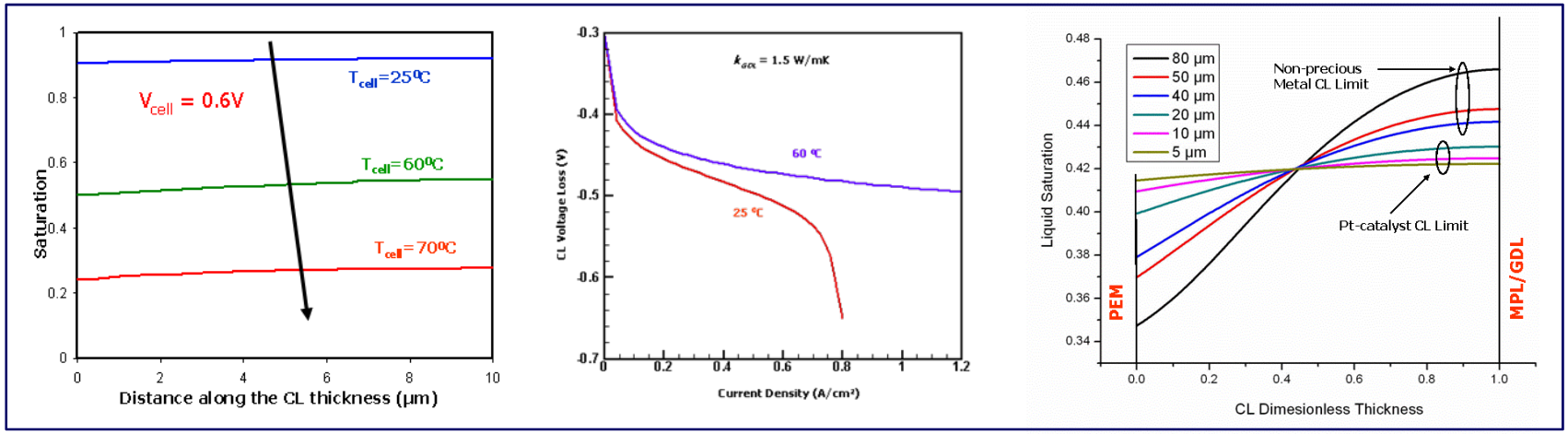

- Low temperature resulting in high liquid water saturation in catalyst layer (limiting current behavior); high temperature leading to enhanced evaporation
- Water vapor condensation in the GDL – a dominant mechanism for mass transport loss
- Capillarity & evaporation – two key design factors for non-precious catalyst layer

Collaborations

- **Eight partner organizations with highly complementary skills and capabilities in catalyst development, electrode-structure design, materials characterization, and catalyst/MEA fabrication:**
  - ✓ Argonne National Laboratory; Brookhaven National Laboratory; Los Alamos National Laboratory; Oak Ridge National Laboratory – *direct DOE contracts*
  - ✓ University of California, Riverside; University of Illinois Urbana-Champaign; University of New Mexico – *subcontracts to Los Alamos National Laboratory*
  - ✓ Cabot Fuel Cells – *subcontract to Los Alamos National Laboratory*
- **Collaborations outside the DOE Hydrogen Program:**
  - ✓ Center for Functional Nanomaterials (Yimei Zhu, Eli Sutter, Ping Liu) – HAADF-STEM imaging and DFT calculations
  - ✓ Case Western Reserve University (Frank Ernst) – chalcogenide microscopy
  - ✓ Northeastern University (Sanjeev Mukerjee) – Se/Ru characterization
  - ✓ University of North Texas (Paul Bagus) – core-shell modeling
  - ✓ University of Virginia (Matt Neurock) – DFT calculations

Future Work

Remainder of FY09:

- Verify performance of Pt/Pd/C catalyst from the scale-up synthesis at Cabot
- Study Pt/Pd/Pd_3Ir, Pd, and Pd-alloy nanorods and nanowires as supports for Pt monolayers
- Develop methodology for making nanostructure-supported PANI-derived catalysts
- Advance the model of non-precious metal catalyst layer; implement findings in electrodes
- Refine synthesis of emulsion/reverse emulsion structures towards smaller Pt nanoparticles
- Complete stability measurements of the best-performing PANI-derived catalyst (PANI-FeCo-C)

FY10:

- Improve methodology for controlled deposition of Pt monolayers on metal nanoparticles to form compact deposits for better particle stability and ORR activity (Pt less prone to PtOH formation)
- Extend Pd-interlayer concept by making suitable supports for a Pt monolayer on refractory metal-based nanoparticles that otherwise adversely affect Pt activity
- Optimize synthesis and performance of heat-treated non-precious metal catalysts, focusing on improvements to durability at high operating cathode potentials
- Investigate detrimental effect of Fe on long-term MEA stability; develop strategies for eliminating iron and/or mitigating its impact on the ionomer
- Reduce mass transport resistance in non-PGM catalysts through the use of novel nanostructures
- Further scale-up and optimize, including optimization of active-phase composition, the spray pyrolysis process for Pt/Pd/C catalyst and, possibly, other viable catalysts
- Continue characterization of atomic structure of two catalyst classes within the project
- Begin long-term stability tests of viable catalysts in the MEA environment

Summary

- Substantial improvement to mass activity of core-shell catalysts, up to 1.2 A/mg_{Pt} at 0.90 V, achieved through introduction of Pd interlayer between different nanoparticle cores and the outer Pt layer
- Much improved stability of PGM nanoparticles obtained in RDE cycling by (i) use of Pd interlayer, (ii) new synthesis approaches, and (iii) deposition of Au clusters on Pt surface ($\Delta E_{1/2}$ shift limited to 16 mV after 50,000 potential cycles)
- Non-precious metal catalysts showing major improvement in ORR activity in RDE and fuel cell testing (OCV up to 1.0 V, volumetric activity in excess of 50 A/cm^3)
- High activity of selected PANI-based catalysts accompanied by good stability (ca. 700 hours in H_2-air cell) and negligible peroxide generation (H_2O_2 < 0.5%)
- Successful industrial scale-up of BNL's Pt_{ML}/Pd/C catalyst accomplished by Cabot; catalyst showing excellent fuel cell performance (0.55 A/mg_{Pt} at 0.90 V)
- Extensive characterization, by X-ray and microscopic techniques in particular, allowing insight into the structure and composition of catalysts, including possible source of activity of non-precious metal formulations
- Project integrated better through close two- and three-way collaborative efforts (e.g. electrode structure development, catalyst fabrication scale-up), testing, characterization, all-project meetings and regularly held discussions
- Several milestones accomplished, some exceeded; most other milestones on schedule; no-go decision made for one catalyst class (surface chalcogenides)

Co-Authors

Brookhaven National Laboratory – **catalysts with ultra-low Pt content**

R. R. Adzic (PI), K. Gong, K. Sasaki, M. Vukmirovic, J. Wang, W.-P. Zhou

University of Illinois at Urbana-Champaign – **chalcogenide-based catalysts**

A. Wieckowski (PI), C. Delacôte, Dr. S. Goubren-Renaudin, X. Zhu

Los Alamos National Laboratory – non-precious **metal catalysts; characterization**

P. Zelenay (Project Lead), J. Bradley, J. Chlistunoff, H. Chung, S. Conradson
F. Garzon, C. Johnston, P. Mukherjee, M. Nelson, G. Purdy, G. Wu

The University of New Mexico – **open-frame catalyst structures**

P. Atanassov (PI), K. Artyushkova, D. Petsev, S. Pylypenko

UC Riverside – **nanostructure catalyst structures**

Y. Yan (PI), S. Alia, K. Jensen

Argonne National Laboratory – **characterization & durability**

D. Myers (PI), M. Ferrandon, A. J. Kropf, X. Wang

ornl – **characterization**

K. More (PI)

Cabot – **fabrication & scale-up**

P. Atanassova (PI), Y. Sun

Supplemental Slides

Cyanamide-Fe-C Catalyst: Synthesis

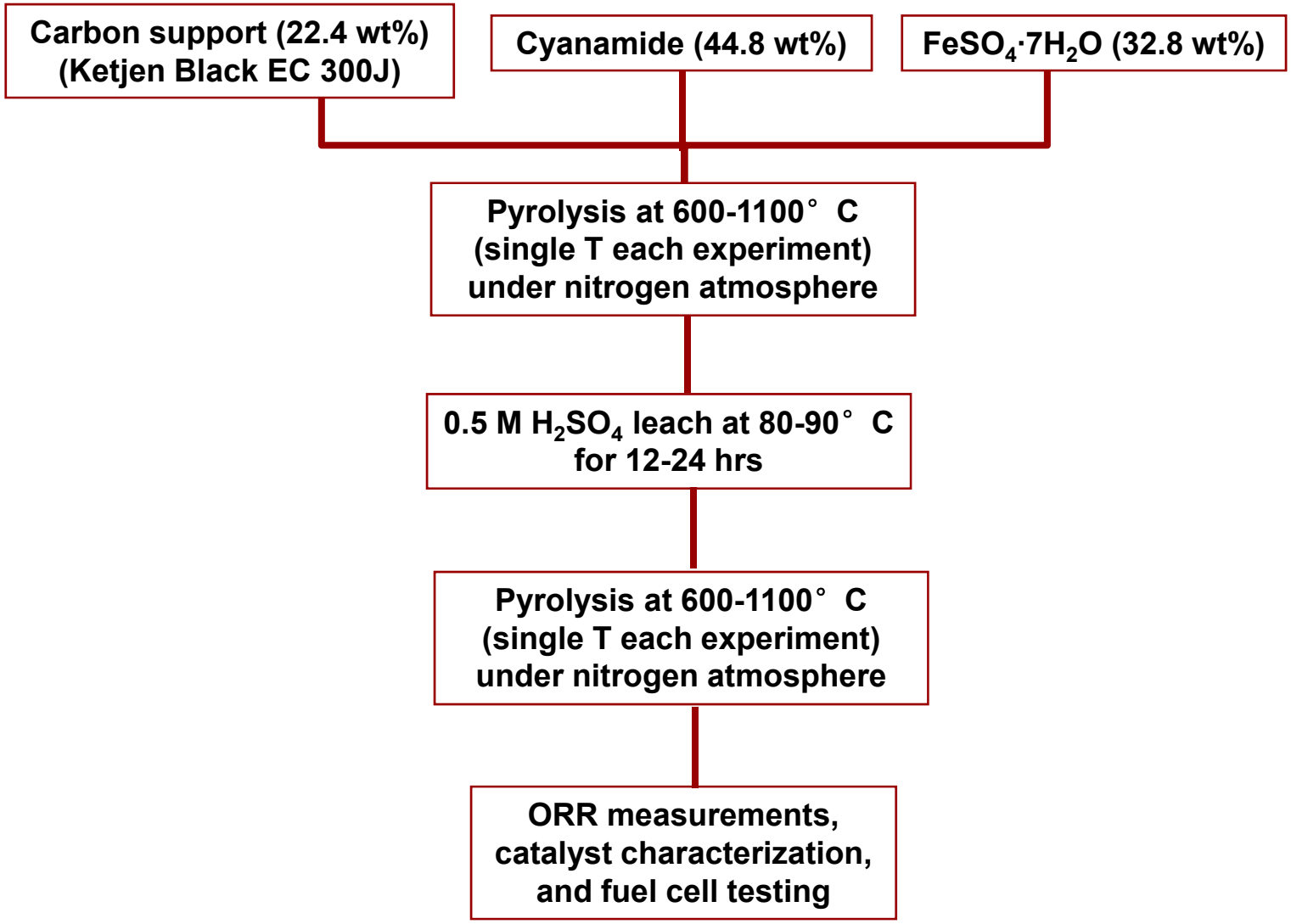

PANI-*Me*-C Catalysts: Synthesis

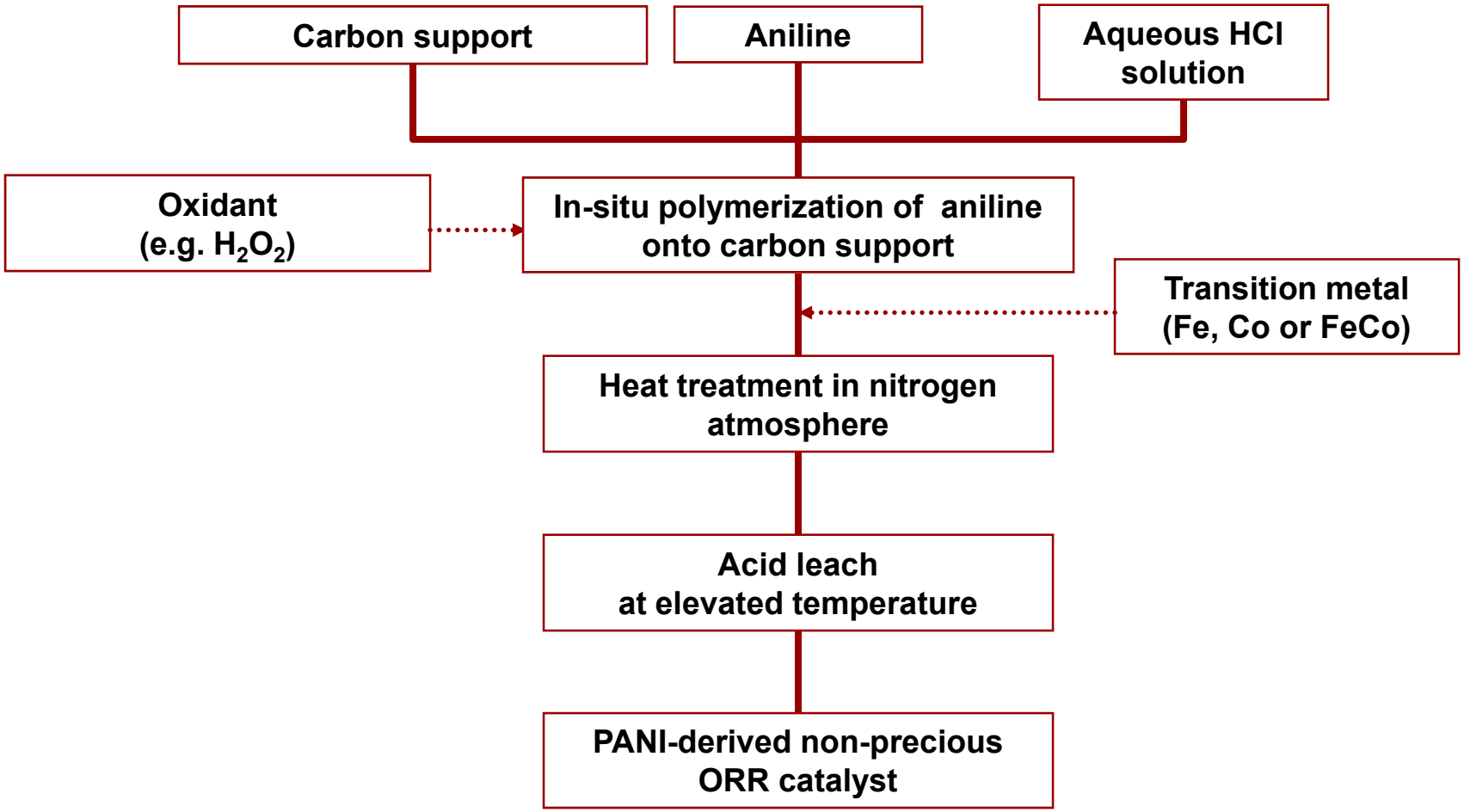

Kinetic Analysis of ORR at PANI-Fe_3Co-C Catalyst

RDE study of ORR

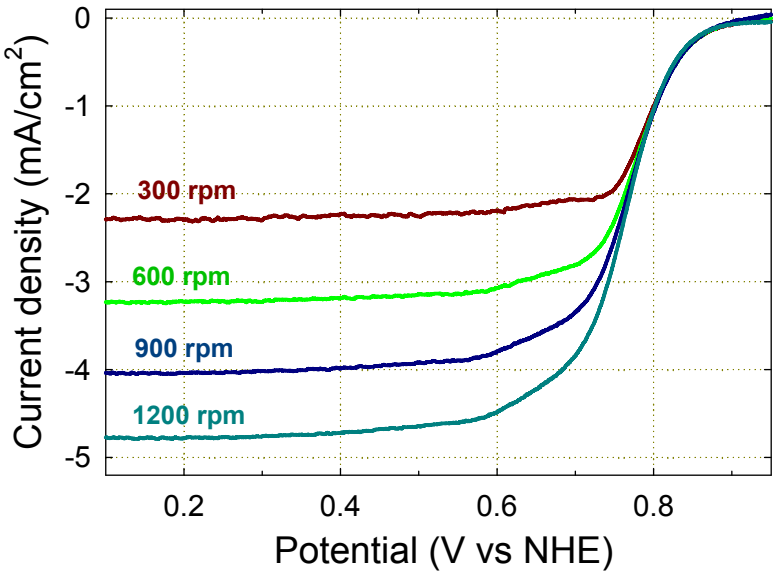

Koutecky-Levich plots

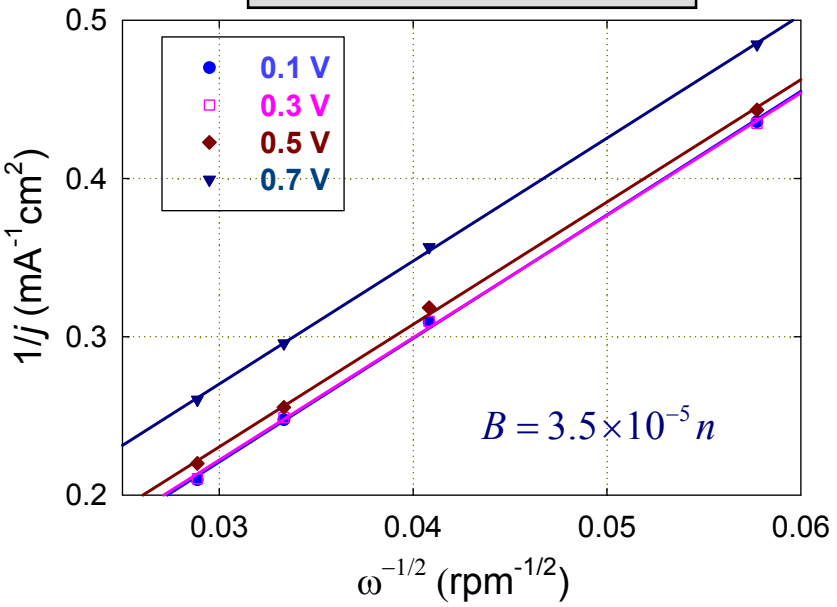

- **Modified Koutecky-Levich equation:*** ***j***, j_k, j_f **and** ***B*** **– overall, kinetic, diffusion limiting current in the film, and Levich constant, respectively**
- **No significant change in** ***n*** **in the potential range from 0.7 to 0.1 V (n ≅ 3.86)**

* Lawson *et al.*, *J. Electrochem. Soc.* 135 (1988) 2247
Wang *et al.*, *J. Electroanal. Chem.* 611 (2007) 87

$$\frac{1}{j} = \frac{1}{j_k} + \frac{1}{j_f} + \frac{1}{(B\omega)^{\frac{1}{2}}}$$

$$B = 0.2nFAC_s(D_s)^{2/3}\nu^{-1/6}$$

Non-precious Catalyst Electrode Model: Catalyst Layer Structure

Bimodal PSD

$$\frac{d\varepsilon_p(r)}{dr} = \frac{1-\varepsilon_{PtC}-\varepsilon_{Nafion}}{\sqrt{\pi}\left\{\ln s_\mu + \chi_M \ln s_M\right\}} \frac{1}{r}\left\{\exp\left[-\left(\frac{\ln(r/r_\mu)}{\ln s_\mu}\right)^2\right] + \chi_M \exp\left[-\left(\frac{\ln(r/r_M)}{\ln s_M}\right)^2\right]\right\}$$

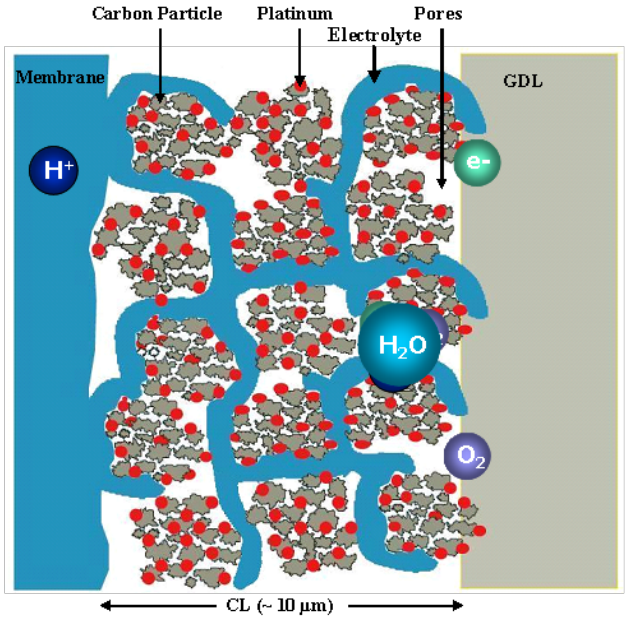

* Based on Eikerling *et al.*, *Fuel Cell Review*, Jan., 2005

PSD — pore size distribution
ε — volume fraction (subscripts: p - pore, PtC - electronic, Nafion® - electrolyte)
r_μ — most probable value of the micro-pore radius
r_M — most probable value of the meso-pore radius
s — spreads of the distribution for micro-pore and meso-pore

Fraction of micro-pores → $f_\mu = \dfrac{\varepsilon_\mu}{\varepsilon_p}$

Ratio of meso- and micro-pores → $\chi_M = \dfrac{\varepsilon_M}{\varepsilon_\mu}$

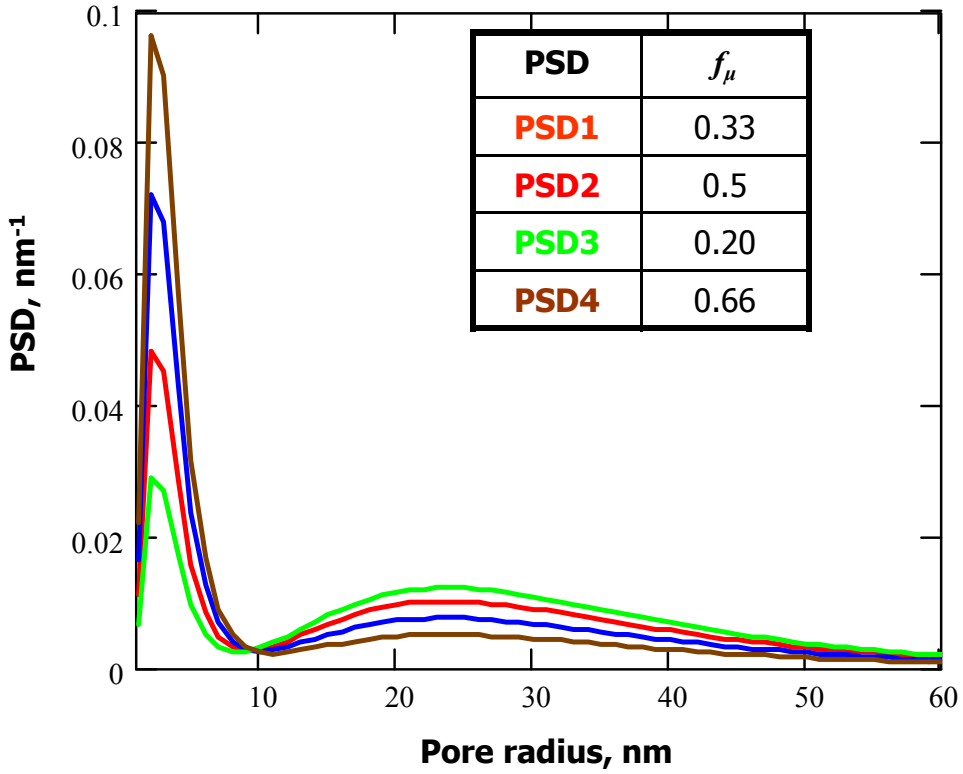

PSD	f_μ
PSD1	0.33
PSD2	0.5
PSD3	0.20
PSD4	0.66

Non-precious Catalyst Electrode Model: Two-phase Constitutive Relations

Capillary pressure:

$$p_c = -\frac{2\sigma\cos(\theta)}{r_c} = p_l - p_g$$

Liquid water saturation:

$$S_r = \frac{1}{\varepsilon_p}\int_0^{r_c} PSD(r)dr$$

Relative Permeability:

$$k_r = \frac{\Lambda\int_0^{r_c} r^2 PSD(r)\,dr}{\int_0^{\infty} r^2 PSD(r)\,dr}$$

- p — pressure (subscript: l - liquid, g - gas, c - capillary)
- k_r — relative permeability
- r_c — capillary radius
- S_r — liquid water saturation
- Λ — electrode structure parameter

Capillary Pressure *vs.* Saturation

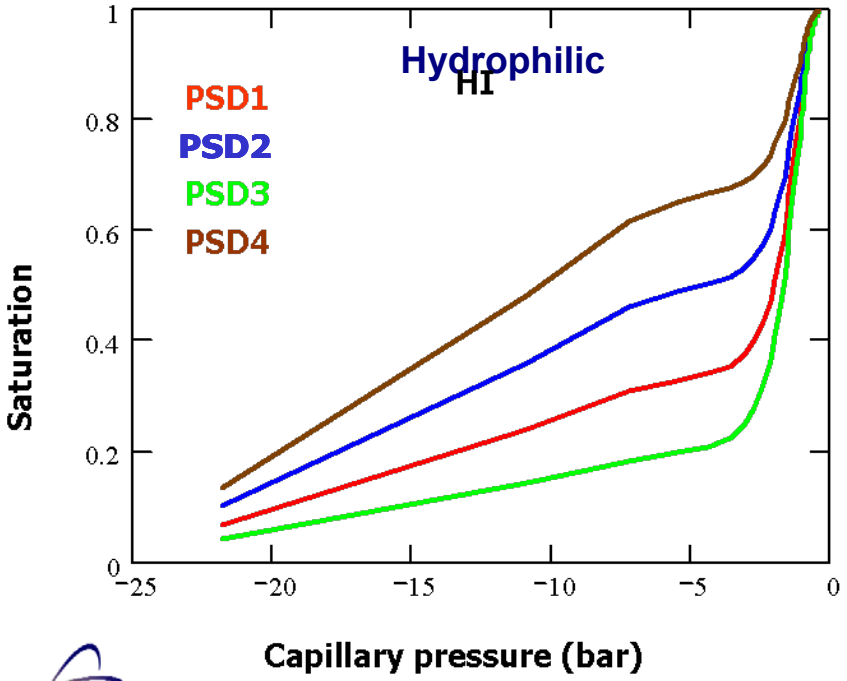

Relative Permeability *vs.* Saturation

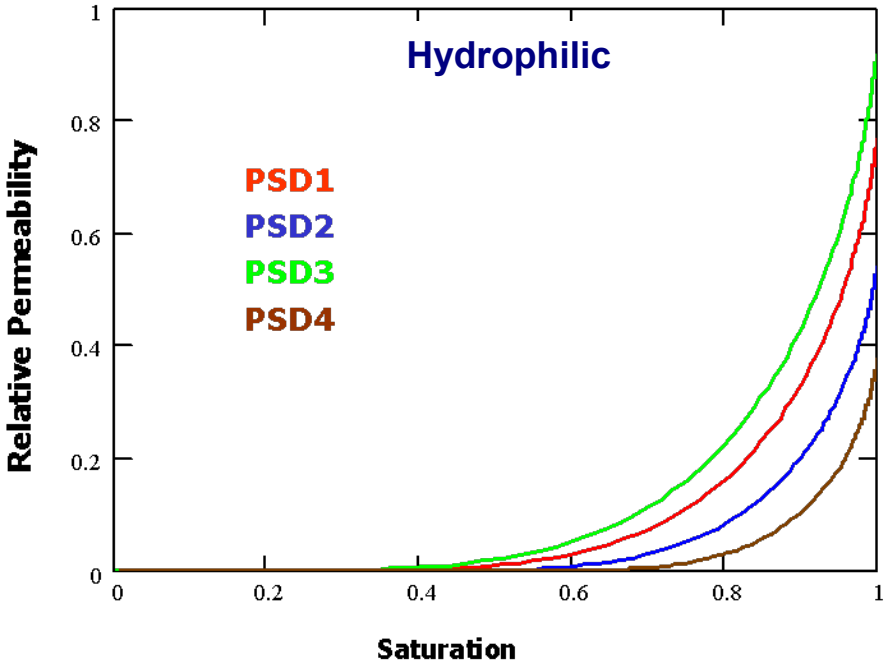

Non-precious Catalyst Electrode Model: Transport Model

Physical model based on water and heat balance

Liquid water transport:

$$-\frac{1}{V_m \mu^l}\frac{d}{dz}\left[K^l(S_r)\frac{dp_l(z)}{dz}\right] = S^l_{ORR} - S_{evap}(S_r)$$

$$J^l\big|_{PEM} = \frac{\alpha I}{F}$$

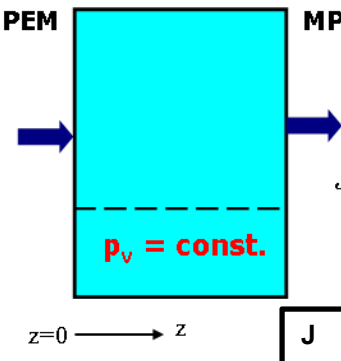

Heat balance comes into play through evaporation

Boundary conditions:

$$J^l\big|_{PEM} = \frac{-\alpha I}{F} \qquad J^l\big|_{GDL} = 0$$

→ **For Hydrophilic CL**

J	—	water flux (sub-/superscript: l - liquid, H_2O - vapor)
α	—	net water transport coefficient from anode to cathode
S_r	—	liquid water saturation
C_{sat}	—	saturation concentration

Water vapor conservation:

$$J^{GDL}_{H_2O} = D^g_{H_2O,eff}\frac{dC_{sat}}{dz} = D^g_{H_2O,eff}\frac{dC_{sat}}{dT}\frac{dT}{dz}$$

Main features:

CL: Liquid-vapor phase transition; water removal from CL to MPL is only through vapor flow

MPL: Vapor flow only due to high entry pressure of MPL

Heat balance equation:

$$q_{tot} - q_{GDL} = h_{fg} J^{GDL}_{H_2O}$$

$$S_{evap}(S_r) = \frac{\beta(S_r)\dot{Q}_{tot}}{h_{fg}}$$

β → heat partition factor
h_{fg} → heat of evaporation

How much of the heat produced in the catalyst layer is utilized for evaporation depending on the GDL thermal conductivity and cell temperature?

Non-precious Catalyst Electrode Model: Electrochemical Performance Analysis

Pore blockage → hindered oxygen transport

$$D^{eff}(S_r) = D^{O_2}\left[\varepsilon_{CL}(1-S_r)\right]^m$$

Catalytic site coverage → reduced ECA

$$a^{eff}(S_r) = a(1-S_r)^n$$

Electrochemical kinetics → Tafel kinetics

$$j = a(1-S_r)^n i_0 \frac{c_{CL}^{O_2}}{c_{ref}^{O_2}} \exp\left(-\frac{\alpha_c F}{RT}\eta_c\right)$$

Oxygen concentration distribution in the CL

$$\frac{d}{dz}\left(D^{O_2}\left[\varepsilon_{CL}(1-S_r)\right]^m \frac{dc_{CL}^{O_2}}{dz}\right) = \frac{j}{4F} = \frac{I}{4F\delta_{CL}}$$

Local oxygen concentration in the CL

$$c_{CL}^{O_2}(z) = c_{Ch}^{O_2} - \frac{I}{4F}\left(\frac{\delta_{GDL}}{D^{O_2}\varepsilon_{GDL}^{1.5}}\right) - \frac{I}{4F}\frac{\delta_{CL}\left[1-\left(\frac{z}{\delta_{CL}}\right)^2\right]}{D^{O_2}\left[\varepsilon_{CL}(1-S_r)\right]^m}$$

Based on the average oxygen concentration in the CL, the *cathode overpotential* (η_c) evaluated as a function of current density and average saturation level in the CL:

Site Coverage **Pore Blockage**

$$\eta_c = -\frac{RT}{\alpha_c F}\ln\left(\frac{I}{a(1-S_r)^n i_0 \delta_{CL}} \cdot \frac{c_{ref}^{O_2}}{c_{Ch}^{O_2} - \frac{I}{4F}\left(\frac{\delta_{GDL}}{D^{O_2}\varepsilon_{GDL}^{1.5}} + \frac{2\delta_{CL}}{3D^{O_2}\left[\varepsilon_{CL}(1-S_r)\right]^m}\right)}\right)$$

Progress in ORR Activity of Non-precious Catalysts: 2008 → 2009

Experiment	Test Conditions	Volumetric Activity at 0.8 V ($A\ cm^{-3}$)		Factor
		2008	2009	
RDE at 25°C	Steady-state 0.5 M H_2SO_4 900 rpm	1.0* (EDA-FeCo-C)	8.3* (PANI-Fe_3Co-C)	8.3
H_2-O_2 fuel cell at 80°C	30 psig 100% RH	5.0* (EDA-FeCo-C)	27* (PANI-Fe_3Co-C)	5.4
			54* (CM-Fe-C)	11

** Catalyst volume calculated using an estimated density of 2.0 g cm^{-3}*

Acknowledgments

- DOE-EERE Hydrogen, Fuel Cells and Infrastructure Technologies Program
- HFCIT Program Managers:
  - Nancy Garland
  - Jason Marcinkoski